Weathering on Coarse Gravel Roads: Modelling Carbon Dioxide Removal in Weathering Processes on Gravel Roads

Miles Barette-Duckworth

A Thesis in The Department of Geography, Planning & Environment

Presented in Partial Fulfillment of the Requirements
for the Degree of Master of Science, Geography,
Urban & Environmental Studies
at Concordia University Montreal, Quebec, Canada

January 2025

CONCORDIA UNIVERSITY

School of Graduate Studies

This is to certify that the thesis

Prepared by: Miles Barette-Duckworth

Entitled: Weathering on Coarse Gravel Roads: Modelling Carbon Dioxide Removal in Weathering Processes on Gravel Roads

and submitted in partial fulfillment of the requirements for the degree of

Master of Science, Geography, Urban & Environmental Studies

complies with the regulations of the University and meets the accepted standards with respect to originality and quality.

Signed by the final Examining Committee:

_____Chair

H. Damon Matthews

_____Examiner

Alex de Visscher

_____Examiner

Eric Galbraith

_____Supervisor

H. Damon Matthews

_____Supervisor

Leonard Sklar

Approved by _____

Chair of Department or Graduate Program Director

_____ 2025 _____

Dean of Faculty

ABSTRACT

Weathering on Coarse Gravel Roads: Modelling Carbon Dioxide Removal in Weathering Processes on Gravel Roads

Miles Barette-Duckworth

As global atmospheric carbon dioxide levels rise, negative emissions strategies are being researched to rapidly capture and store these emissions. Enhanced rock weathering as a negative emissions strategy has a strong focus on research on agricultural applications, however, the construction and maintenance of gravel roadways represents an under-researched potential form of weathering. This research examines the contributions of gravel roadways in West Bolton, QC to the reduction of atmospheric carbon dioxide levels through chemical weathering. A model was produced using Stella modeling software to simulate the atmospheric carbon dioxide transformation through weathering of the roadway material in the study area. A sieving analysis was performed to determine both the change in rock particle size over time and for the calculation of the available surface area of the road material. A weathering analysis was performed using road material sampled from the roadway and rainwater captured within the study area. Alkalinity readings as the concentration of $CaCO_3$ were obtained during the weathering analysis and using particle size distribution for the surface area along with the annual rainfall data, weathering rates for all three sample sites were calculated. The weathering rates were found to be $1.36x10^{-6}$ mol/m^2, $2.25x10^{-6}$ mol/m^2, and $4.11x10^{-6}$ mol/m^2. Of critical influence on the weathering rate was the volume of annual rainfall. Model simulations using the results of the sieving and weathering analysis found that the carbon transformation using the analysis results corresponded to the modeled results using reference rates. Factors influencing the modeled carbon transformation were found to be mechanical fracturing from annual daily car passage and maintenance frequency over timescales of ten years. This study begins the research on gravel roads as a negative emissions strategy and produces a model that can inform road management decisions.

Acknowledgements

I would like to first and foremost acknowledge my wife, Agunik Mamikonyan, for her endless support, encouragement, and concessions made to allow me the time and space to finalize my thesis during our parenting journey.

To my children, Tiffany, Theodore, and Thatcher. I hope that this serves as an example that the pursuit of learning and higher education does not need to follow a traditional path, and I hope you will all find your unique paths when the time comes.

Damon Matthews and Leonard Sklar, thanks for bearing with me while I grew my family, and your continuing support when returning to finish this project. Your guidance and excitement for the research was invaluable to this project. It has been a privilege to have you both as supervisors.

Sarah Turner, it is thanks to your initial encouragement and introduction to Damon that got this whole master's started. I wouldn't have been here without your initial encouragement.

The late John Rhicard, thank you for your willingness to provide information about road maintenance at the early stages of this project. Without your wealth of knowledge about the eastern Townships (particularly its roads and quarries), this research would not have been possible.

To my late grandparents, Clare and John Duckworth, thanks for choosing to retire in West Bolton. The memories I made encouraged me to explore and seek a deeper understanding of the last place you called home.

Table of Contents

List of Figures

List of Tables

Chapter 1 – Introduction

Problem Situation

The level of atmospheric carbon dioxide has increased rapidly in the last century, increasing more than 50% since the beginning of the industrial revolution (National Oceanic and Atmospheric Administration 2022). Negative emissions strategies are being explored to mitigate the effects of climate change and rapidly reduce the amount of atmospheric carbon dioxide. Without a reduction in atmospheric carbon dioxide levels along with a process in place for their continued removal by 2050, the impacts of climate change may be unavoidable (May and Rehfeld 2019).

While the impacts of climate change are becoming more apparent, enhanced rock weathering is one among many negative emissions strategies being explored. Enhanced rock weathering in the simplest of explanations is the process of breaking and spreading rock over the earth's surface so it can be degraded chemically by rainwater. The physical breakdown of rock material is critical to the effectiveness of enhanced weathering as it increases the surface area for the weathering reaction to act upon. As I will demonstrate in the literature review, the exploration of this strategy has rarely left the process of agriculture. Nevertheless, humans are practicing enhanced rock weathering at a global scale with the construction and maintenance of gravel roads. Despite the ubiquity of this practice, the effects on atmospheric carbon dioxide remain an area poorly researched.

Considering Canada has several hundred thousand linear kilometers of unpaved roadways, amounting to nearly forty percent of Canadian road infrastructure, there is a significant amount of unintentional enhanced weathering occurring that is unaccounted for as a negative emissions strategy (Statistics Canada 2009).

As will be discussed in greater detail in the literature review section, the adoption of new practices that reduce atmospheric carbon levels faces many hurdles in adoption. This research therefore focuses on an existing process and aims to assess the impact of roadway construction on atmospheric carbon levels and determine what changes can be made to increase the impact of this practice.

Research Objective and Questions

The primary objective of this research is to determine whether silicate rock weathering occurring on gravel roadways contributes meaningfully to the reduction of atmospheric carbon dioxide levels, over short timescales. The hypothesis for this research is as follows; if the minerals present on gravel roads are easily weathered and are subject to chemical weathering conditions, then a decrease in composition of labile elements present in the mineral and an increase in alkalinity (as $CaCO_3$) in water from the chemical weathering reaction will be detectable.

The first question this research aims to answer is to define which roadway factors influence weathering. Modeling the weathering process will permit a myriad of inputs to be adjusted to determine which factors affect the weathering of rock materials and ultimate carbon dioxide transformation.

A second question that the study seeks to answer is what surface area is present on a roadway in the study available for weathering. Sieving analysis allows for accurate quantification of the available surface area for weathering reactions on the roadway by providing a breakdown of the particle sizing in a roadway, allowing for the total surface of all particles to represent the available surface area.

Third, this research intends to determine a localized weathering rate for the various materials used on roadways in the study area. A weathering simulation using roadway material, assumed to be silicate minerals, and the result of the sieving analysis permits for weathering rates localized to the study area to be determined.

A secondary objective of the research is to establish a tool in the form of a model for roadway managers to employ as a factor in deciding which materials are best suited for roadway construction and allowing for decisions to be made considering the impacts on atmospheric carbon dioxide. Determination of roadway factors and material-specific weathering rates in the study area allows for a secondary objective of the research to be fulfilled.

Research Site

The research presented was performed in West Bolton, QC. This research site was chosen for several factors, the first being that the roadway construction manager (John Rhichard) is known to the author and was willing to supply information about the roadway construction for this study. A second reason for this study location is the availability of a suitable place for rainwater collection, which as discussed later requires a long period for the device to be fixed in

place. West Bolton also presents an area with a significant unpaved road network of approximately 90 linear kilometers. The study area is shown in the following figure.

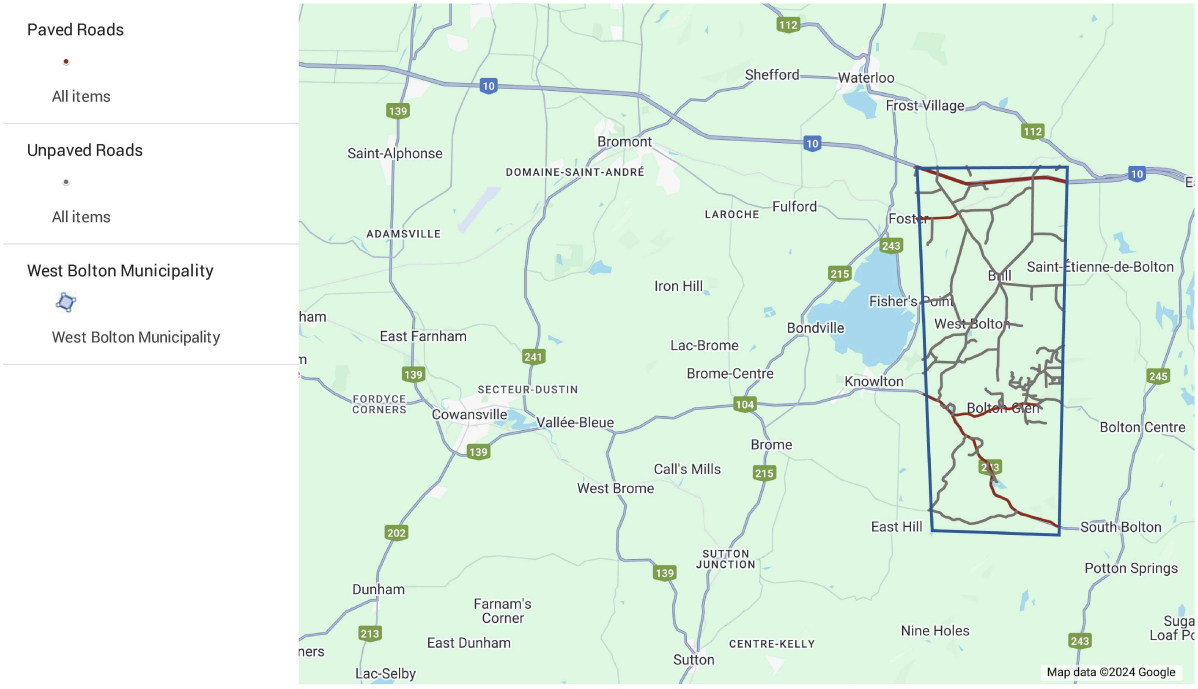

Figure 1 Location and road network of the study area (West Bolton, QC)

Chapter 2 – Literature Review

As high and ever-increasing levels of atmospheric carbon dioxide are one of the primary drivers of climate change, many strategies to remove this atmospheric gas are being explored. There is a significant focus on the generation of new technologies, alongside the investigation of strategies to enhance earth-system processes to remove and sequester carbon dioxide in long-term carbon pools. Over a geological timescale, the chemical breakdown of rocks has been a long-term moderator of atmospheric carbon dioxide (Kasting 1984). This occurs when atmospheric carbon dioxide reacts with rock material and is transformed in a process called chemical weathering. The alkalinity increase is subsequently transported in an ionized form by earth systems processes for storage in the world's oceans (R D Schuiling and Krijgsman 2006). Enhanced weathering is a proposed strategy to reduce atmospheric carbon dioxide and mitigate the effects of climate change whereby the natural process of weathering is sped up with human intervention. Anthropogenic intervention includes a reduction of the size of easily weathered rocks to increase the available surface area for weathering, and subsequent distribution of the rocks over the earth's surface.

The incorporation of enhanced weathering into farming practices has been an area of significant research as organic activity has been shown to increase weathering rates compared to a laboratory setting (R D Schuiling and Krijgsman 2006; Roelof Dirk Schuiling 2017). Applications of weatherable material to croplands has been shown to significantly increase soil inorganic carbon when compared to untreated croplands (Haque, Santos, and Chiang 2020). While this increased efficiency of incorporation into agriculture does have many benefits, there

are also uncertainties and potential negative side effects (Edwards et al. 2017a). Additionally, a lack of suitable land has been cited as one of the main barriers to implementation (Moosdorf, Renforth, and Hartmann 2014). Modifying existing behaviors is a strategy that has been successful at increasing the frequency of pro-environmental choices, which raises the question of what anthropogenic actions could be slightly modified to incorporate the concept of enhanced weathering (Heberlein 2013).

The construction and maintenance of unpaved roads present an opportunity to modify existing behavior and incorporate enhanced weathering as a pro-environmental choice. The practice of building and maintaining unpaved roads is an example of unintentional enhanced weathering; fresh rock materials are exposed through mining and then reduced in size and spread over large areas of the earth's surface. These two activities enhance the earth systems weathering cycle by increasing the amount of weatherable exposed rock on the earth's surface. In Canada alone, unpaved roads represent 626,600 km of roadway, while worldwide there are estimated to be over 7 million km of unpaved roads (CIA 2017; Statistics Canada 2009).

In the following sections, an overview of the factors that affect weathering will be presented and weathering as a method to remove carbon dioxide from the atmosphere will be examined. Following this, gravel road construction principles and the potential for carbon dioxide removal will be described. Lastly, potential confounding factors that could affect carbon dioxide removal will be investigated.

Weathering

Broadly defined, weathering is the breakdown of rock by earth systems processes. Weathering can be classified as either mechanical or chemical. Mechanical weathering refers to the breakdown of rocks due to mechanical forces, while chemical weathering refers to chemical reactions that transform minerals present in rocks into new chemical compounds.

Many mechanical forces can cause weathering. Water-driven weathering occurs when water is driven by thermodynamic forces toward a lens of ice applying pressure against a mineral surface. When temperatures reach between -3 and -6 C the water supply to the ice lens is restricted, while pressure increases causing the rock to fracture (Hallet 2006). Expansive force can result from infiltrating plant roots or salt crystal formation left behind as water evaporates. Lastly, the application or removal of compressive forces (from overlying soil, tectonic plates, or other materials) can result in rock breakage (Earle 2015).

Chemical weathering occurs when minerals in rock react chemically with their environment. Broadly speaking chemical weathering is categorized into two main categories: silicate weathering and carbonate weathering. Carbonate weathering is generally discarded as a climate mitigation measure as it does not transform atmospheric carbon on geological timescales, and in some cases can be considered a short term or even source of atmospheric carbon (Lehmann et al. 2023). Silicate weathering on the other hand is viewed as a climate mitigation measure, as it transforms atmospheric carbon into dissolved bicarbonate where it can be transported to oceans and stored over geologic timescales (Earle 2015). This can take the form of oxidation, hydrolysis, or dissolution (Earle 2015). Dissolution is of special interest, as dissolved

carbon dioxide (as carbonic acid) in water can react with rock to form free bicarbonate ions (Earle 2015). These ions are then carried to oceans, where they are used by marine animals. When the marine animals perish, their shells containing the transformed carbon dioxide fall to the ocean floor where they remain until subducted into the earth's mantle (Kantola et al. 2017).

Chemical Weathering Rates

Weathering rates are an area of research that has raised academic interest for some time. In 1981 Colman found that weathering is not constant in time as previous research had assumed, by determining that the rate of weathering is reduced over time (Colman 1981). Pre-dating this is the work of Berner, who determined that the presence of water containing carbonic acid was not solely responsible for mineral weathering (Berner 1978). Many other factors affect mineral dissolution including temperature, available reactive surface area, pH, the presence of organic acids, and many others (Bray et al. 2015; Kump, Brantley, and Arthur 2000).

As with most chemical reactions, the amount of the reagent present will exert some control over the quantity of products produced. Chemical weathering follows this principle however the amount of reagent present in chemical weathering reactions is determined by the exposed surface area. The grain size, along with the surface area available for reaction has been shown to influence the weathering rate (Israeli and Emmanuel 2018; Montserrat et al. 2017). Furthermore, the surface texture and surface mineral composition has been shown to affect the weathering rate (Taksavasu et al. 2024)

Advancement in research instruments allows for new research to occur as shown in a study on pH dependency on weathering reaction rates in boreal regions. In this research, it was

observed that weathering rates are faster at the edges of the rock being weathered, that certain minerals are released through weathering at changing rates (Mg and Fe are freed more rapidly than Al for the mineral Biotite), and that overall, the type of organic material present affects the reaction rate, with weathering rates decreasing as pH increases (Bray et al. 2015). More recently, it was found that soils below a pH level of 5.8 may not be suitable for enhanced weathering efforts, and soils with a pH below 6.3 would require consideration of acids other than carbonic acid reacting with minerals (Dietzen and Rosing 2023).

Weathering has also been shown to not simply be from chemical reactions. Mechanical detachment of microscopic grains is also a factor in the weathering rates, contributing to as much as 50% of the weathering rate (Israeli and Emmanuel 2018). However, factors like mineral composition, the surface distribution of the mineral composition, the surface roughness of the rock, and the boundaries between similar mineral clusters affect weathering rates (Israeli and Emmanuel 2018).

As has been briefly shown, the rate at which weathering occurs can be affected by many factors, all of which can vary regionally. Owing to this, the weathering rate is regionally specific. Studies using the dissolved ion composition in water in catchment areas show that the estimated weathering rate can vary both within a catchment and between catchment areas, demonstrating the extent to which weathering varies regionally (Jiang et al. 2018; Millot et al. 2002).

Enhanced Weathering

Enhanced weathering can be defined as the enhancement of the earth-systems process of chemical weathering through anthropogenic action. As previous research has shown, the chemical weathering reaction is influenced by the quantity of available surface area. Enhanced weathering therefore seeks to increase the surface area available with the goal of speeding up the chemical weathering reaction. This anthropogenic intervention intends to increase the removal of carbon dioxide from the atmosphere by chemically weathering greater quantities of rock.

Perceptions

For the majority of individuals, there are strong chances that enhanced weathering as a method to reduce atmospheric carbon dioxide is not known. A study in the UK revealed that only 6.5% of survey participants had substantial knowledge of weathering, while over two-thirds of participants had never heard of enhanced weathering (Pidgeon and Spence 2017). Enhanced weathering is supported by those who are familiar with the concept (Pidgeon and Spence 2017). More recent analysis of perceptions highlight that most survey favor populations industrialized regions, with surveyed populations confirming earlier findings of a favourable opinion and a low awareness of novel carbon dioxide technologies (Smith et al. 2024). Despite this favorable opinion, there are many valid concerns over implementation such as the long-term responsibility and maintenance of the implementation program, unknown long-term effects, and potentially unknown effects on the larger ecosystem (Edwards et al. 2017a; Lawford-Smith and Currie 2017; Pidgeon and Spence 2017).

Not all side-effects of enhanced weathering are cause for concern, as one of the main projected long-term effects of weathering is the eventual increase of alkalinity (and corresponding reduction in acidity) of the world's oceans. This occurs when the products of chemically weathered rock (bicarbonate ions) are transported through dissolution in water to the oceans (Edwards et al. 2017a; Lawford-Smith and Currie 2017; Roelof Dirk Schuiling 2017; Taylor et al. 2016). Overall, with a favorable public perception and the reduction of ocean acidification as an additional benefit, enhanced weathering does appear to be a viable solution to remove carbon dioxide from the atmosphere. Despite this viable solution, more research can be done regarding the unknown effects of implementation in new areas, and an effective long-term management strategy can be put into place.

Effectiveness

Worldwide, the carbon flux from rock weathering amounts to less than 3% of our current carbon dioxide emissions from fuel (Taylor et al. 2016). Enhanced weathering fluxes are small still, recent estimates, which rank the United States as the largest contributor to carbon reduction through enhanced rock weathering, quantify this removal as 0.03Mt of CO_2 annually out of 2,200 Mt active deliberate global carbon reduction efforts estimated globally (Smith et al. 2024). Forest management (afforestation/reforestation) accounts for the large majority of these active efforts, with technological undertakings representing only ~1.35Mt of carbon reduction annually (Smith et al. 2024). Many studies propose enhanced weathering as a safe way to effectively increase this percentage (Taylor et al. 2016). A significant portion of the research consulted suggests that for weathering to be enhanced, rocks need to be reduced in size to increase the weathering reaction surface area, with proposed sizes ranging from silt to sand (10 μm – 256

μm) (Strefler et al. 2018; Taylor et al. 2016). This size reduction is necessary to maximize effectiveness, as the reduction in particle sizing increases the available surface area for weathering.

Many different negative emissions techniques have been suggested to mitigate the effects of climate change and rapidly reduce the atmospheric carbon dioxide concentration. One such strategy suggests that an application of 5 kg/m^2-year of 10 μm diameter easily weathered rock over an area of 20 million km^2 could allow us to lower the atmospheric carbon dioxide concentration by 30-300 ppm by 2100, exceeding what can be removed through current earth-systems processes (Taylor et al. 2016). Another researched application finds that depending on the rock type and the factors influencing the carbon dioxide removal, 0.54 - 1.02 tons of carbon dioxide per ton of rock could be sequestered if all the rock was weathered (Moosdorf, Renforth, and Hartmann 2014). Should the weathering reaction continue to material depletion, a 4 mm layer of easily weathered rock powder applied on all landmasses could consume all the atmospheric carbon dioxide, including carbon dioxide from human activity (R D Schuiling and Krijgsman 2006). It would be reasonable to question how this efficient removal of carbon dioxide could be achieved, and what implementation strategies have been proposed.

Proposed Implementations

The focus of the research surrounding implementation possibilities of enhanced weathering has primarily been implementation in tropical and sub-tropical areas. Implementations in these aforementioned areas are proposed in conjunction with agricultural practices. The geographical focus is a direct result of the temperature dependence of weathering

rates, while the focus on agricultural practices is driven by the pH dependence of the weathering rate (Dietzen, Harrison, and Michelsen-Correa 2018; Roelof Dirk Schuiling 2017).

Tropical and sub-tropical regions present excellent geographical areas for weathering primarily for two reasons. Firstly, these regions would be the most effective in terms of temperature, as the climate is optimal for weathering to occur (Roelof Dirk Schuiling 2017). The climate is deemed to be ideal for weathering in these regions as there is ample precipitation and temperatures remain warm year-round. Secondly, weathering in tropical regions presents an ideal area as the limiting factor for chemical weathering is primarily the lack of rock material available for weathering (Edwards et al. 2017a). This lack of weatherable material is a consequence of the high weathering rates experienced in these regions, as all weatherable material has been weathered.

Agriculture presents an excellent implementation activity as the organic activity in the soils produces many organic acids which speed up the weathering of rocks that have been incorporated into the soil (Roelof Dirk Schuiling 2017). Vegetation traditionally dominates tropical regions in the form of rainforests or agricultural land, which presents a constant source of organic activity and organic acids (Edwards et al. 2017a). Additionally, the incorporation of rock dust into the soil also reduces the carbon dioxide produced by agriculture by replacing agricultural lime (often used as a fertilizer that releases carbon dioxide) and can improve productivity by improving the mineral composition of soils (Dietzen, Harrison, and Michelsen-Correa 2018; Edwards et al. 2017a; Taylor et al. 2016). The cost of rock weathering practices in croplands has been quantified to cost between $160-$190 in North America and Europe, while

these costs are cut in half due to differences in labour and fuel costs in Asia and South America (Beerling et al. 2020).

While weathering in tropical and sub-tropical agricultural practices is an excellent implementation method, little research has been performed exploring weathering in non-agricultural contexts. There may be many reasons for this lack of exploration, including the ease of incorporation into farming practices as those practices are prevalent in the tropical and sub-tropical regions, however, to best meet climate targets all options should be explored (Edwards et al. 2017a).

Following the thought of agriculture being an industry to easily incorporate enhanced weathering, the question as to what other industries enhanced weathering could be incorporated into is a logical one to pose. At its base, enhanced weathering is as explained earlier, reducing the size of easily weathered rocks and spreading them on the earth's surface. Unpaved road construction is an industry that meets the exact basic tenants of weathering: rocks are made smaller and spread over the earth's surface, however, the exact compositions of the minerals in the rock material vary by location, as road design manuals often recommend that materials be sourced from what is locally available (Skorseth and Selim 2000). Furthermore, it incurs no direct cost when compared to rock weathering implementations in agricultural practices, as the rock weathering outcome is a side effect of the main objective of roadway construction. In the following section, we'll explore briefly the unpaved road construction practices.

Road Design

Unpaved road construction practices vary according to local regulations and the type of road being constructed. As an example, in British Columbia, the provincial guidelines on unpaved road construction have different specifications based on the purpose and expected speed requirements of the road (B.C. Ministry of Transportation 2007). Despite the different specifications, commonalities exist among regions and road types; depth requirements and the size of the rock used for surface and base layers are standardized based on the region (B.C. Ministry of Transportation 2007; Skorseth and Selim 2000).

The following example is an effort to demonstrate how to estimate the volume of rock present on unpaved roadways in British Columbia using the specifications for roadway construction found in literature published by the provincial government. British Columbia was chosen as an example as the government-supplied construction manual was the most current found at the provincial level. The following formula will be used for this volume calculation:

$$Total\ Rock\ volume = (Road\ Length * Road\ width * Layer\ depth) * (1 - Porosity)$$

The surface layer of roads (150 mm depth) and the specified minimum road width (7 m) in British Columbia are multiplied to produce the profile of the roadway (B.C. Ministry of Transportation 2007). The profile can then be multiplied by the total length of unpaved roads in British Columbia (22,900 km), giving us a volume of 24,045,000 m^3 (Statistics Canada 2009). This volume is then multiplied by one minus a porosity factor of 0.4 (meaning 60% of the space

is occupied by the rock, this porosity factor is based on a range of findings by Frings, Schüttrumpf, and Vollmer (2011)) to obtain the total volume of rock present.

This estimation yields a volume of 14,427,000 m^3 of rock that is currently present in the surface layer of unpaved roads in British Columbia alone. Considering that there are more than 7 million kilometers of unpaved road worldwide, the rocks used for these roadways could play some part in the weathering process, and at minimum present an excellent industry where enhanced weathering could be incorporated into existing practices (CIA 2017).

It is important to note that the rock sizes used in gravel roads are significantly larger than those in the enhanced weathering potential researched in agricultural practices, as unpaved roads can use sizes ranging from 0.074 mm to 15 cm depending on the layer of road in question and the regional specifications (B.C. Ministry of Transportation 2007; Skorseth and Selim 2000; The Pennsylvania State University 2018). Attention then turns to potential factors that can conflict with the weathering reaction on gravel roads.

Potential Conflicts

Despite the potential benefits that enhanced weathering presents, potential conflicts exist. The first potential conflict is the emissions generated from the crushing and transport of the rock material to the roadways for weathering. A second potential conflict specific to roadways is the use of dust suppressants.

Emissions are produced by almost every anthropogenic action taken. Roadway construction is no exception, with emissions embedded in the mining, breakdown, and transport

of minerals from the quarry to the roadway, and from machinery during construction and maintenance. Research into applications of enhanced weathering has revealed that the emissions from mining and rock breakdown to a size of 1mm are negligible, with the main source of emissions stemming from vehicular emissions during transport from the quarry to the weathering site (Moosdorf, Renforth, and Hartmann 2014). Recent research confirms these findings, by confirming that the energy demand is offset by the weathering potential of particles when the rocks are milled to fine sizes (Kantzas et al. 2022). Despite the primary emissions resulting from transport, the transportation would have to exceed 5000 km to offset the carbon dioxide reduction from the particles' lifetime of enhanced weathering (Moosdorf, Renforth, and Hartmann 2014). Contrary to this finding, with emissions of 2.66 kg of carbon dioxide per liter of diesel fuel and a fuel efficiency of 2.50 km/l for the average dump truck, a 10-kilometer trip would produce 10.64 kg of carbon dioxide ("Emission Facts: Average Carbon Dioxide Emissions Resulting from Gasoline and Diesel Fuel (EPA420-F-05-001)" 2005). Most gravel roadway construction manuals encourage the use of nearby, readily available minerals, as the cost of transport would cause construction budgets to skyrocket (The Pennsylvania State University 2018; Skorseth, Ried, and Heiberger 2015). As such, is unlikely that emissions from transportation would approach the amount of carbon dioxide removed from the spread of rock material during construction and maintenance.

Gravel roadway construction and maintenance do present a potential conflict, as there are emissions embedded in every maintenance event. These emissions have not yet been compared in research consulted to the potential removal caused by the addition of new weatherable material.

A second potential conflict is the use of dust suppressants in gravel roadway construction. The use of dust suppressants is necessary to preserve roadway integrity and prevent gravel loss (Monlux, Mitchell, and Monlux 1989). Chlorides, are the most commonly applied dust suppressants due to their hygroscopic properties, allowing the roadway surface to be at a constant moisture level to reduce dust levels (Skorseth, Ried, and Heiberger 2015). No research was found describing the effects of chlorides on the chemical weathering of minerals.

Summary

Research into the application of enhanced weathering has focused on tropical and sub-tropical areas and the incorporation of exceedingly small-sized rock particles in agricultural practices. While this research has demonstrated excellent opportunities for enhanced weathering to be incorporated into current agricultural practices, there has not been much exploration beyond this application. Unpaved roads present a large volume of rock that is currently being subject to enhanced weathering unintentionally, and this research intends to demonstrate further enhanced weathering applications and their potential contribution to the global atmospheric carbon dioxide budget.

Gravel roadways presenting an unintentional form of enhanced weathering, along with the many spatially distinct factors that affect weathering rates create a unique chance for modeling the atmospheric carbon dioxide removal potential of a road area. As the literature consulted has demonstrated, this type of research has not yet been performed, it is an exciting opportunity to improve the understanding of factors influencing atmospheric carbon dioxide and

build a relevant model that can be used by geoscientists and infrastructure planners alike to understand the effects of building and maintaining unpaved roads.

Chapter 3 – Methodology

Stella Model

Introduction

As part of this research, I developed a model using the Stella modeling software developed by ISEE Systems. Modeling is a useful research tool as it can be used to inform and predict real-world systems to a degree of accuracy. The Stella software was chosen for its reputable use as a modeling software for systems dynamics, and despite proprietary language the ability for models to be translated into the open-source language R using StellaR (Naimi and Voinov 2012). The graphical interface allows for communication of the systems involved.

The objective of this endeavor was to create a model of the transformation of atmospheric carbon dioxide through chemical weathering (carbonation), using a roadway as the material available for weathering. The purpose of the model was to produce a decision-making tool for roadway managers to allow for consideration of the impacts on atmospheric carbon that a given roadway rock material would provide. The ability to include carbon transformation as a factor in the decision of roadway management can allow for pro-atmospheric carbon reduction decisions.

The model uses established background rates of weathering for specific minerals, to allow for easy substitution of established rates with in-situ rates. Lacking any real-world analysis, background rates could be used as a proxy should the approximate rock composition be known.

Model Description

Roadway Volume

The Stella model developed begins with the calculation of the roadway volume, using the roadway characteristics of length, width, depth, and porosity. This simple calculation allowed me to establishment of the volume of rock material available for weathering.

Porosity is assumed to be 0.4, as roadway construction guidelines such as the Highway Maintenance Guidelines and Level of Service Manual (Alberta Transportation 2000) do not advocate for compaction of material and recommend scarification to increase traction during the winter months, while others such as Highway Maintenance and Operations Handbook will recommend compaction with a blade (McDonald and Sperry 2014). Lacking consistent guidelines on roadway compaction, I took the assumption of a porosity value of 0.4 as it fits within the reference range of 0.1 to 0.5 (Frings, Schüttrumpf, and Vollmer 2011).

Gravel roadways require maintenance due to the lack of long-term roadway integrity, therefore functions were added to account for material lost as dust and new material added during maintenance events (McDonald and Sperry 2014). I used reference rate of loss of 1 ton annually lost per daily car passage per mile (0.56kg/m per vehicle) from the Gravel Roads Maintenance and Design Manual to derive the following loss calculation (Skorseth, Ried, and Heiberger 2015).

$$\frac{0.56\text{kg/m} *. \text{Road Length (m)} * \text{Annual daily car passage}}{\text{Gravel density } (1800\ \text{kg/m}^3)}$$

Incorporating the road volume allowed me to model for the annual gravel loss rate for a given road volume and the material lost as dust.

I deemed that the gravel added to the system during a maintenance event was equivalent to the gravel lost as dust, with the assumption that the roadway is returned to its original state. However, due to varying maintenance requirements such as roadway traffic, and climatic conditions, roadway maintenance events may occur at varying intervals annually, so I introduced a variable to allow for the specification of the annual maintenance frequency. Allowing for maintenance frequency to be specified creates a system wherein the roadway volume decreases between maintenance events.

Particle Size Breakdown

Following the modeling of the roadway volume, the volume is broken down by particle (rock) sizing, to obtain the percentage volume by particle size. This breakdown is modeled using the recommended composition percentages by particle size (seven increments) found in various road construction and maintenance handbooks (The Pennsylvania State University 2018; Kennebec County Soil and Water Conservation District and Maine Department of Environmental Protection Bureaus of Land Resources and Water Quality 2016; Skorseth, Ried, and Heiberger 2015). When creating the model, I assumed each particle to be a perfect sphere, which allowed for volume and area calculations.

As I established in the description of the roadway volume modeling, the volume of the roadway fluctuates between maintenance events. This mechanical breakdown of roadway particles is modeled such that larger particles are reduced in size, fall into all lower percentage increments, and continue until the lowest increment, whereby the particles are lost as dust at the volume specified in the roadway volume modeling. The following figure taken from the Stella model demonstrates this particle mechanical fracturing flow.

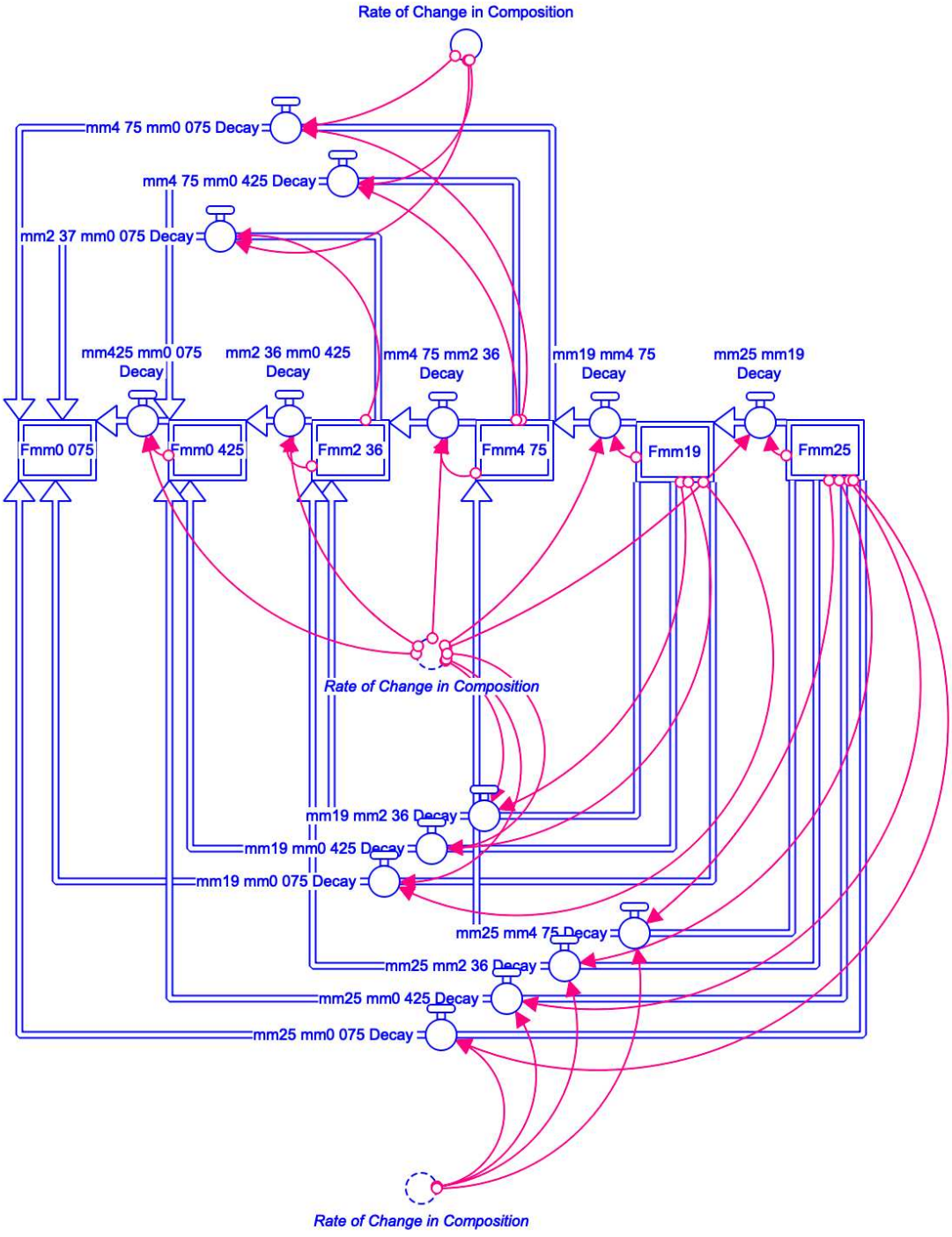

Figure 2 - The flow of particles after breakdown from mechanical forces

Mechanical fracturing can occur between 5% and 43% of the material depending on the forces applied by the car passage, however, across a roadway surface the breakdown percentage was found to be between 36% and 43% (Berthelot and Carpentier 2007). The model uses the lower end of this range (36% or 0.36) as the annual decay factor for particle size decrease. This is represented as the "Rate of Change in Composition" in Figure 2 above.

During maintenance events, material added is done in the ideal reference percentages. The resulting influence on the model is such that the percentage composition of the roadway by particle size is ever-changing, leading to a constant fluctuation of available surface area for weathering. The fine particles see an increase in percent composition over time, while the remainder of the increments present an ever-decreasing percent composition. Should maintenance events not occur, total weatherable material is reduced as it is either transformed via weathering or simply transported outside of the study area.

Using the specified particle sizing composition percentages, along with the volume of each particle increment, I established the count of each particle using the following equation:

$$\frac{Percent\ of\ Roadway\ per\ particle\ size}{Volume\ of\ particle}$$

With the count established, I was then able to determine the surface area per particle size, by multiplying the count by the surface area of a given particle. This provided me with the available surface area for the weathering reaction to occur.

Carbon Transformation

Once I established the total available surface area for weathering, I used this to model the carbon transformation. The calculation of the transformation uses the following equation:

$$Available\ Surface\ Area * Material\ weathering\ rate * mol\ ratio\ for\ reaction\ * Molecular\ weight\ CO_2$$

$$m^2 \quad * \quad \frac{mol}{m^2 * month} \qquad * \qquad \frac{mol\ CO2}{mol\ material} \qquad * \quad \frac{kg}{mol}$$

Where the weathering rate can be specified depending on the rock material used for the roadway. The mol ratio (2) is derived from the reaction of carbonic acid (present from dissolved carbon dioxide in water) with silicate rock material producing bicarbonate ions:

$$CO_2 \ + \ H_2O \rightleftharpoons H_2CO_3$$

$$2H_2CO_3 + CaSiO_3 \rightleftharpoons Ca^{2+} + 2HCO_3^- + \ H_2SiO_3$$

The result of which is the total amount of atmospheric carbon dioxide transformed by weathering. The mol ratio can be adjusted to match the weathering rate of the roadway material used (silicate or carbonate minerals), and the corresponding carbonic acid reaction. The model also allows for the weathering contribution by grain segment to be visualized.

Web Model

I began working on web version of the Stella model as part of this project. The aim was to increase accessibility to the model and allow for ease of integration into roadway management decisions. Despite this ambitious objective, I abandoned this portion of the project as the programming language used to write the mathematics (JavaScript) behind the model is poorly suited for complex mathematical uses, resulting in inaccurate results. The incomplete project can

be viewed at https://app.milesbd.ca/, however, the project is not finalized and requires the mathematics to be re-written in a programming language suited for complex mathematical operations.

Roadway Rock Particle Size Distribution Analysis

A significant component of the model is the mechanical breakdown of rock material applied to a roadway. As I previously mentioned, the decrease in particle size increases the amount of fresh available surface area for weathering. The purpose of the inclusion of this as part of the research was to determine how rock source, rock composition, and time since application onto the roadway affected the rock particle breakdown. The rock source, rock composition, and time since application were provided to me by the roadway manager for the sample site, and permission was granted to collect and process roadway samples.

Rock Particle Collection Procedure

To perform this analysis, I sampled three roadway locations representing three roadways resurfaced within a two-year period using rock material from different origins were selected. Sample location 1 was resurfaced using rocks quarried from a mountain source and was added to the roadway in 2018. Sample location 2 was added to the roadway in 2019, from a ground excavation site. Lastly, similar to sample location 2, sample location 3 was added to the roadway in 2019, with the difference being that the source of the rock material was from a quarried riverbed. The following figure identifies the sample locations.

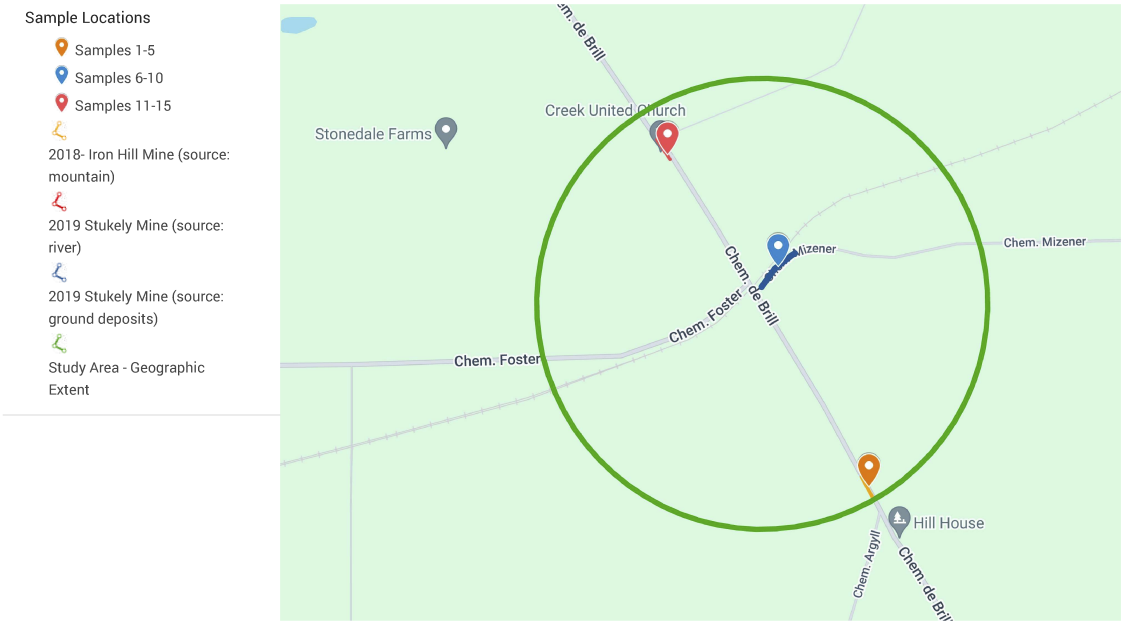

Figure 3 Sample site geographical locations

From each sample location, I selected five sample sites spaced 1 meters apart. At each of these sample sites, I collected a sample of roadway weighing more than 1kg from each of the lane center (LC), roadway center (RC), and roadway edge (RE). My intent in sampling three sites across the roadway is to account for differences in force application from car passage. I dug each sample to a minimum depth of 10cm to obtain an appropriate amount of compacted material. I then placed each sample into a labeled Ziplock bag to not lose any fine material before processing. I performed the collection of samples on August 28, 2020.

Sample Processing and Analysis

I performed sample processing using a set of sieves, and a sieve shaker. The sieve shaker used was a Cenco Meinzer Catalog No. 18480. The sieves used were of sizes 26.5mm, 6.7mm, 4mm, 2mm, 0.42mm, and 0.0075mm with a fines-catching plate placed at the bottom of the

stack. I secured the stack of sieves to the shaker table using rope. The following image showcases my complete sieve and shaker table setup.

Figure 4 Shaker Table and Sieves setup

With the shaker table and sieves in place, I started the rock analysis of the rock size breakdown by weighing the sample in the Ziplock back. I recorded this weight in grams using a scale and then poured the sample into the top of the sieve set on the shaker table. I then weighted empty bag to ensure accuracy of the starting weight of the material. Following this, I turned on the sieve shaker table, shaking the sieve stack for five minutes on intensity setting 8. After

shaking I disassembled the shaker stack weighing and recording the full weight of each sieve before emptying the material contents. I then recorded the sieve weight after emptying the sample to obtain accurate material capture by sieve diameter. To determine the errors in accuracy in grams I subtracted the initial weight, and the sum of all recorded materials caught by the sieve gradations. The scale used to weigh the material was a calibrated CGoldenwall scale, model CNA403, with an accuracy of 0.1g, and a maximum capacity of 5000g. Data Tables 1 through 3 hold the recorded data.

Weathering Analysis

A weathering analysis was performed using simulated conditions, whereby samples were saturated in rainwater collected from a site within the same geographical area. The saturation of the samples was done to ensure that the rock specimens remained in optimal conditions for weathering. The change in alkalinity throughout the analysis was recorded at 24-hour intervals and used as a proxy for carbon transformation through the reaction of weathering from carbonic acid and the silicate rock material (Edwards et al. 2017b).

Water Collection Procedure

Drawing from the methods used by Rastegari Mehr, Keshavarzi, and Sorooshian (2019) I collected rainwater at a height of approximately 100cm from the ground surface. I used a non-reactive polyethylene circular container with a diameter of 91.4cm and a wall height of 17.5cm. The rainwater I collected was from precipitation between September 7th, 2019, and October 2, 2019, at a site approximately 4.5km from the sample locations. I chose this rainwater collection site as rainwater collection was performed over a long period requiring the collection setup to be

in a fixed location, and this was a residential property where I was permitted to put the rainwater collection setup. The rainwater collection site is shown in the following figure.

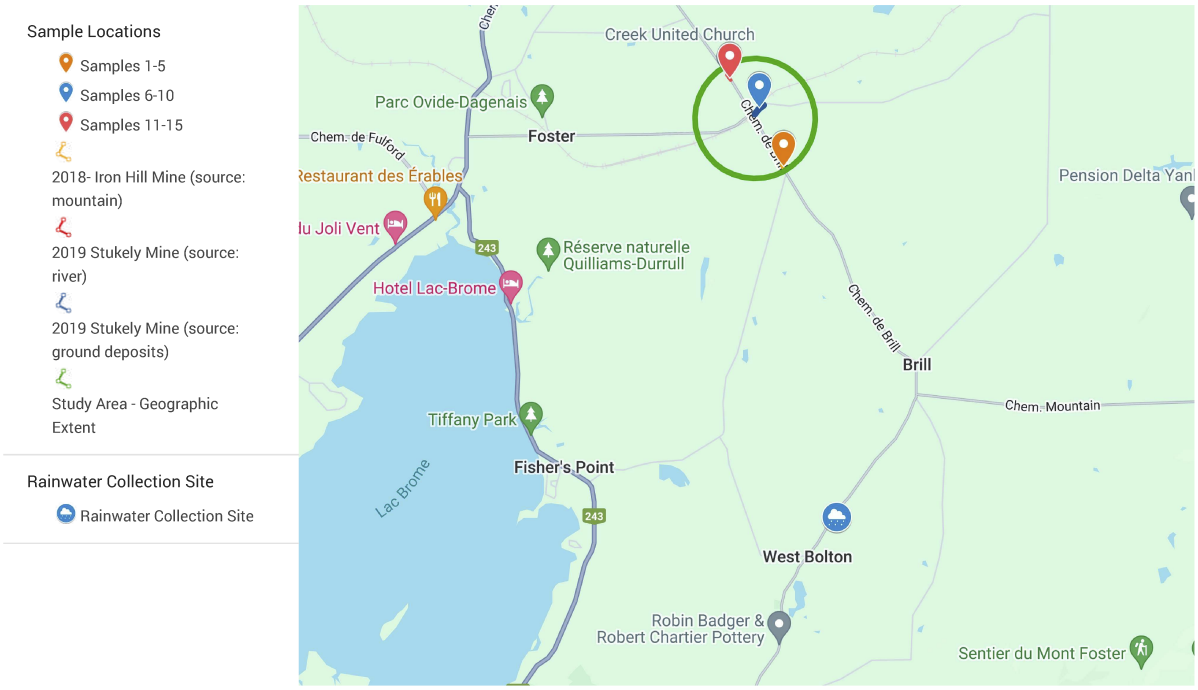

Figure 5 Geographical Location of Rainwater Collection Site

The rainwater collection container was emptied three times during the collection period. For each emptying, I used a rubber and PVC hand siphon in conjunction with a polyethylene funnel (fitted with a brass screen to ensure the removal of any large particulate matter or debris) and emptied the rainwater into sealable polyethylene pails for storage. Prior to emptying the rainwater into the storage pails, I rinsed the equipment with a portion of the rainwater collected to avoid any contamination. In total, I collected and stored two pails of 10L and 20L respectively.

Sample Processing and Analysis

Prior to rock sieving analysis, I removed randomly selected samples from each sample location (sample sites 3, 8, and 14). From each sample site, I took and thoroughly combined samples of a quantity between 110g and 135g from each road center, road edge, and lane center sub-sample sites, and placed the samples into a rainwater-rinsed polypropylene sealable container, forming a total of nine per-sample site specimens for analysis. The mixture of road center, road edge, and lane center samples was necessary to obtain results that represent the entire roadway. I rinsed the containers with rainwater to ensure that any contamination present comes from the rainwater.

To each specimen, I added approximately 165mL of rainwater, promptly inverting the container with the lid firmly closed to allow for full and immediate saturation. I also prepared three control samples of only rainwater, with approximately 200mL of rainwater present in each. I loosened the container lids to allow for any gas effusion to occur but kept the lids atop the containers to prevent any water loss due to evaporation. The containers were stored for the duration of the analysis in a sunlight-free area.

At 24-hour intervals, for 5 days, I tested for pH, Total dissolved solids (TDS), Electrical conductivity (EC), temperature, and total alkalinity tests and recorded the results using a calibrated Hanna Instruments Model 98129 Combo pH/Conductivity/TDS Tester and a calibrated Hanna Instruments Model HI775 Freshwater Alkalinity Checker (along with Hanna Instruments alkalinity reagents). The instrument used to calculate alkalinity had a range from 0 to 500 ppm for alkalinity as $CaCO_3$ and a resolution of 1 ppm. Each alkalinity test required an extraction of 10 ml from the specimen, and I did not add any additional rainwater as the

specimens remained saturated from the amount of rainwater initially added. All other tests were performed by submerging the probe into the solution, and I thoroughly rinsed and dried the probe between samples using distilled water. I weighed and recorded each sample before and after sampling. I performed the weighing with the same scale I used during the roadway rock particle size distribution analysis (Cgoldenwall scale model CNA403).

To determine the amount of carbon dioxide transformed, I used the following equations as a reference:

Weathering

$$H_2O + CO_2 \rightleftharpoons H_2CO_3$$

$$2H_2CO_3 + CaSiO_3 \rightleftharpoons Ca^{2+} + 2HCO_3^- + H_2SiO_3$$

Sequestration

$$HCO_{3^-} \rightleftharpoons H^+ + CO_3^{2-}$$

$$Ca^{2+} + CO_3^{2-} \rightleftharpoons CaCO_3$$

The alkalinity measurement is therefore taken to be equivalent in number of moles to the amount of HCO_3^-, assuming that the system is in instantaneous equilibrium when the measurement is taken. The same assumption was recently used in a quantification of CO_2 removal in Malaysia (Larkin et al. 2022).

To convert from the change in concentration in ppm of alkalinity to a weathering in mol/m^2, several calculations need to be performed. Firstly, I needed to convert the alkalinity in ppm to mol/L of $CaCO_3$. I performed this using the following equation:

$$\frac{ppm}{1000 * Molar\ Mass\ \mathrm{CaCO_3}}$$

Once I determined the change in concentration in mol/L, the change in only units of mol needed to be isolated. I did this by dividing the change in concentration over the mass (for this study, the rainwater is assumed to have a density of 1 kg/L) and obtained the change in concentration of $CaCO_3$ in moles. As the reaction is taking place on a specific surface area of material, the available surface area the reaction occurred over can be established using the rock particle distribution breakdown as discussed earlier. First, I determined the volume of the roadway by particle size, noting that the calculation is performed per particle increment resulting in 6 values, according to the following formula:

$$\frac{mass\ of\ gravel\ (g)}{gravel\ density\ (g/m3)} * Particle\ size\ breakdown\ percentage$$

Once I knew the volume of the roadway, I established the particle count using the lower particle diameter from the range (e.g. for the range of 26.5mm to 6.7mm, I took the diameter of 6.7mm to obtain the particle volume). Using the dimensionless particle count, I then multiplied by the surface area of the corresponding grain size to obtain the surface area available for weathering present by particle size in the specimen during analysis, noting that it is again producing 6 values.

$$\frac{Volume\ of\ roadway\ for\ particle\ size}{\frac{4}{3}\ \Pi\ r^3} * 4\Pi\ r^2$$

Then I took the sum of the surface area available for weathering present per particle size to obtain the total surface area acted upon during the analysis, which provided a weathering rate in mol/m^2.

Chapter 4 – Results

Stella Model

The model was run using roadway-specific information from the municipality of West Brome; 90km of linear unpaved roads, with an average roadway width of 8m for the unpaved roads (DMTI Spatial Inc. 2018). The roadway depth was assumed to be the standard of 0.25m, and the porosity was assumed to be 0.4. The maintenance interval was assumed to be annually. Particle size distribution was taken from a sample analysis coming from one of the resurfacing contractors, certifying that the supplied material passed the required standards (see supplementary data 1). Using a reference silicate weathering rate found by Brantley for rock in a similar geographical region of 4.17e-06 mol / m^2 * year, and a mol ratio of 2 (derived from the silicate weathering reaction), the model was run (White and Brantley 2003).

The result of the model yielded an annual transformation of approximately 51.57kg of atmospheric carbon dioxide, with a five-year transformation of 257.87kg. Running the model with the same parameters, but on a longer timescale of ten years saw a total transformation of 792.30kg (see following figures).

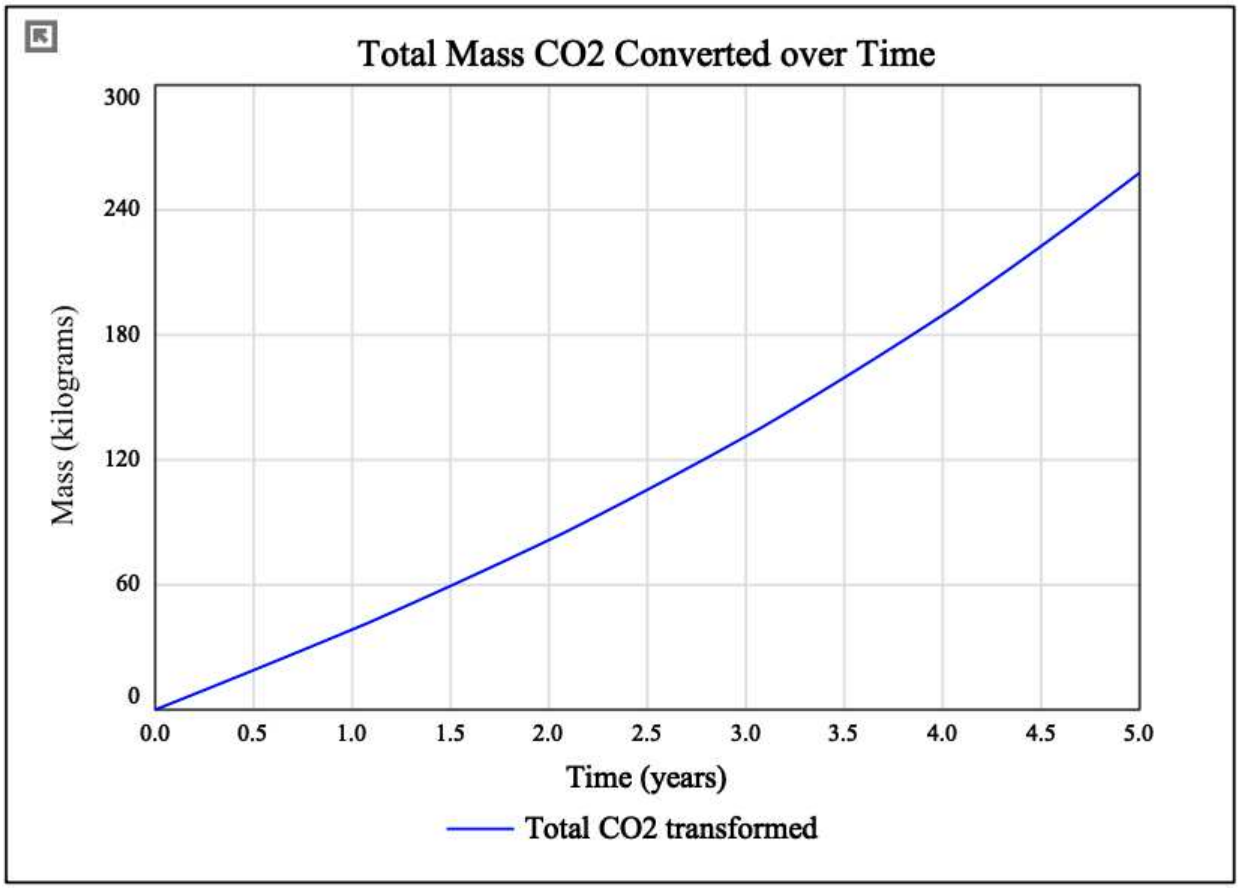

Figure 6 Model results for a 5-year simulation

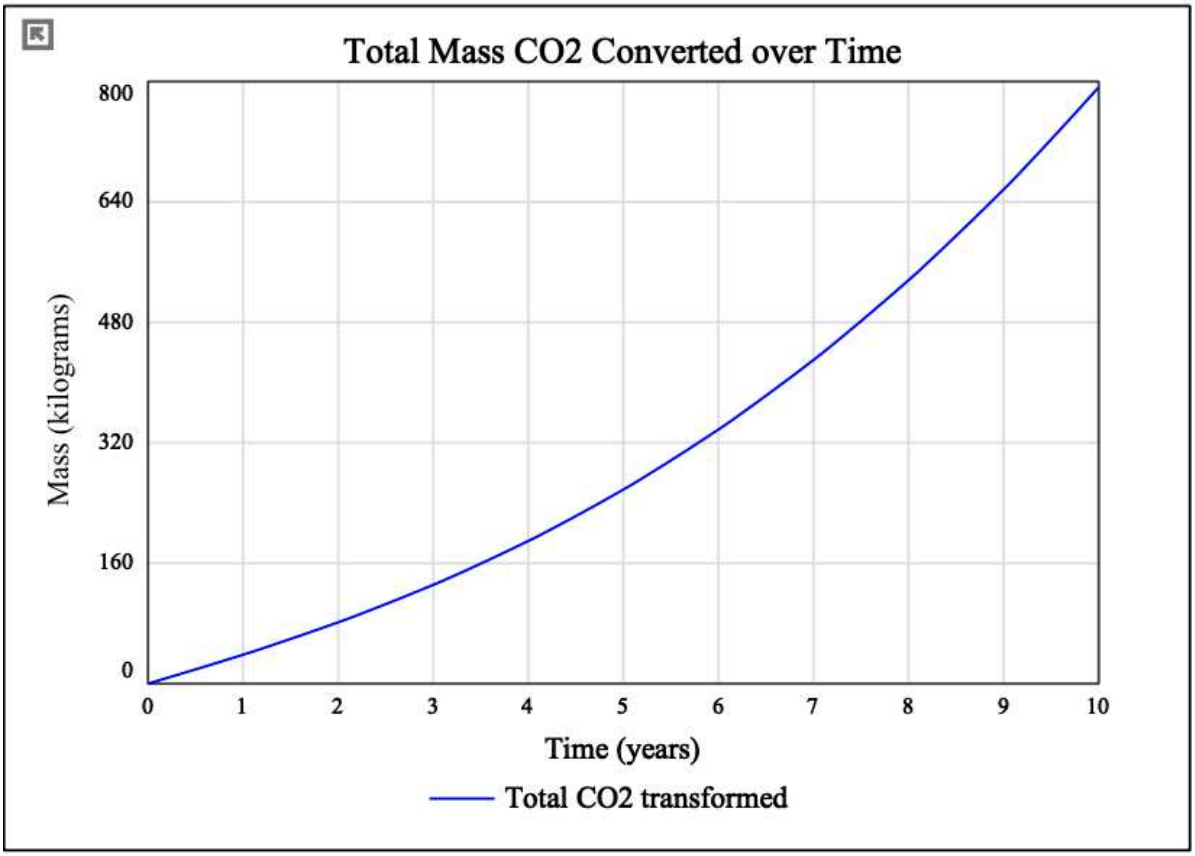

Figure 7 Model result for a 10-year runtime

As both runs establish, there is a slight exponential increase in the amount of carbon dioxide transformed over time. The size distribution changed over time to indicate an accumulation of smaller rock particles, ultimately increasing the available surface area for weathering to occur.

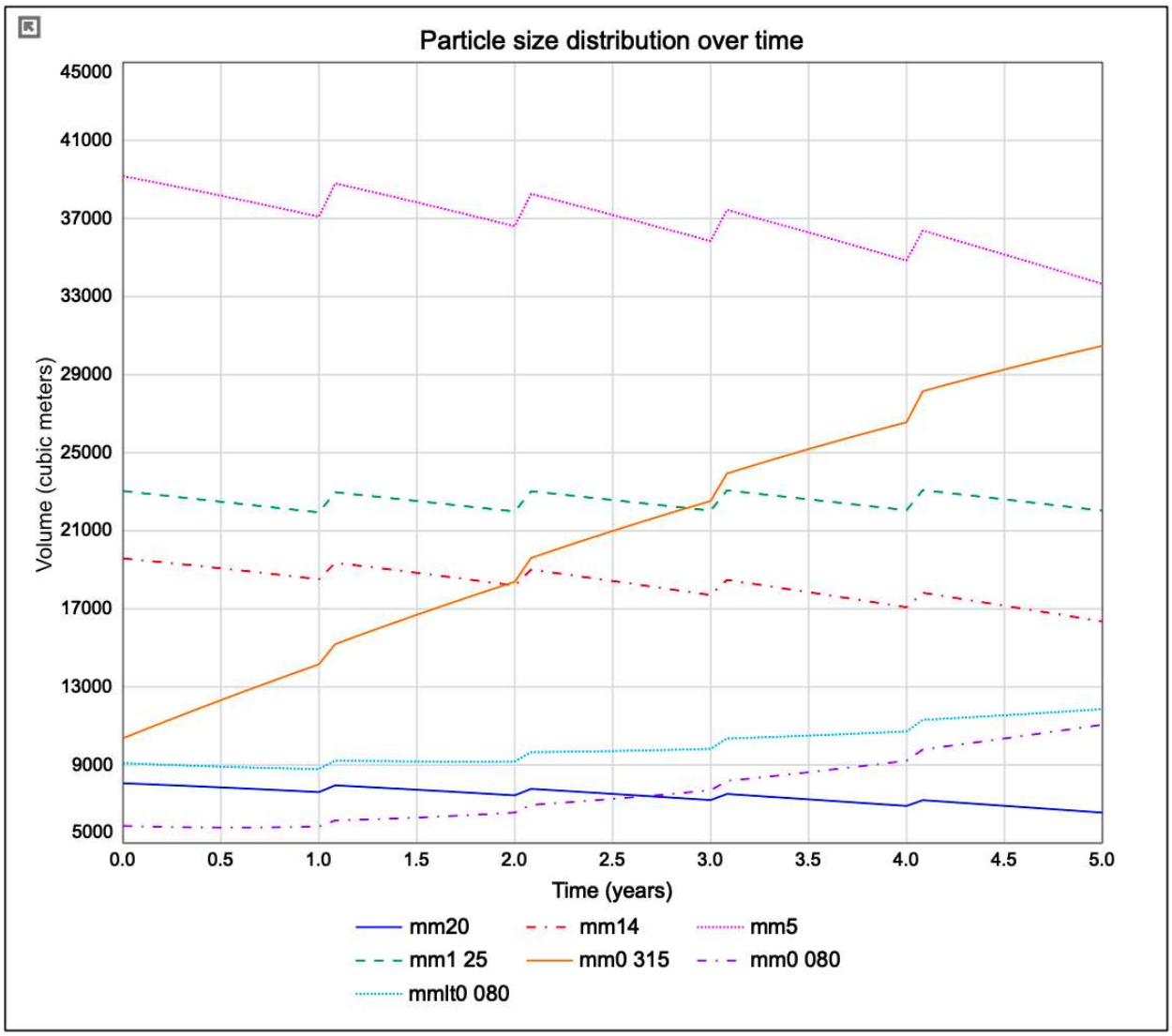

Figure 8 Particle size distribution over time for 5-year runtime

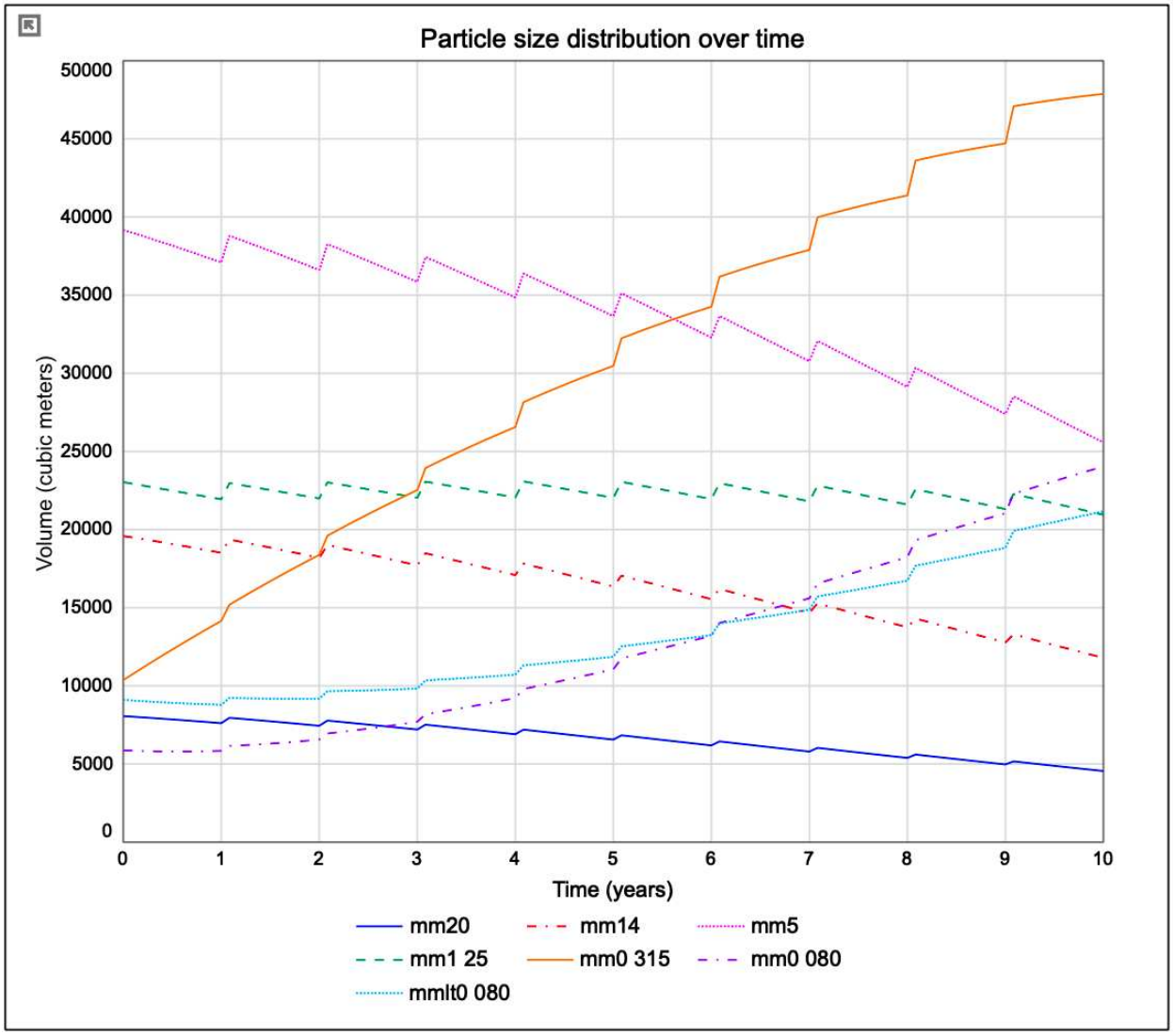

Figure 9 Particle size distribution over 10-year runtime

Adjusting maintenance frequency from once per year to four times per year had little effect on the five-year and ten-year runs, increasing the mass converted by only 4.81kg (262.68kg total) and 14.97kg (807.28kg total) respectively. However, doubling the annual daily car passage rate saw a significant increase in carbon dioxide transformed of 64.64kg and 390.76kg over a five-year and ten-year simulation respectively.

Roadway Rock Particle Size Distribution Analysis

The rock distribution analysis showed variations in size breakdown between both time since application and type of material. Furthermore, when comparing the modeled rock size breakdown after one year to location 1 which was resurfaced a year prior to sample collection, a variation between modeled and real-world distribution is found.

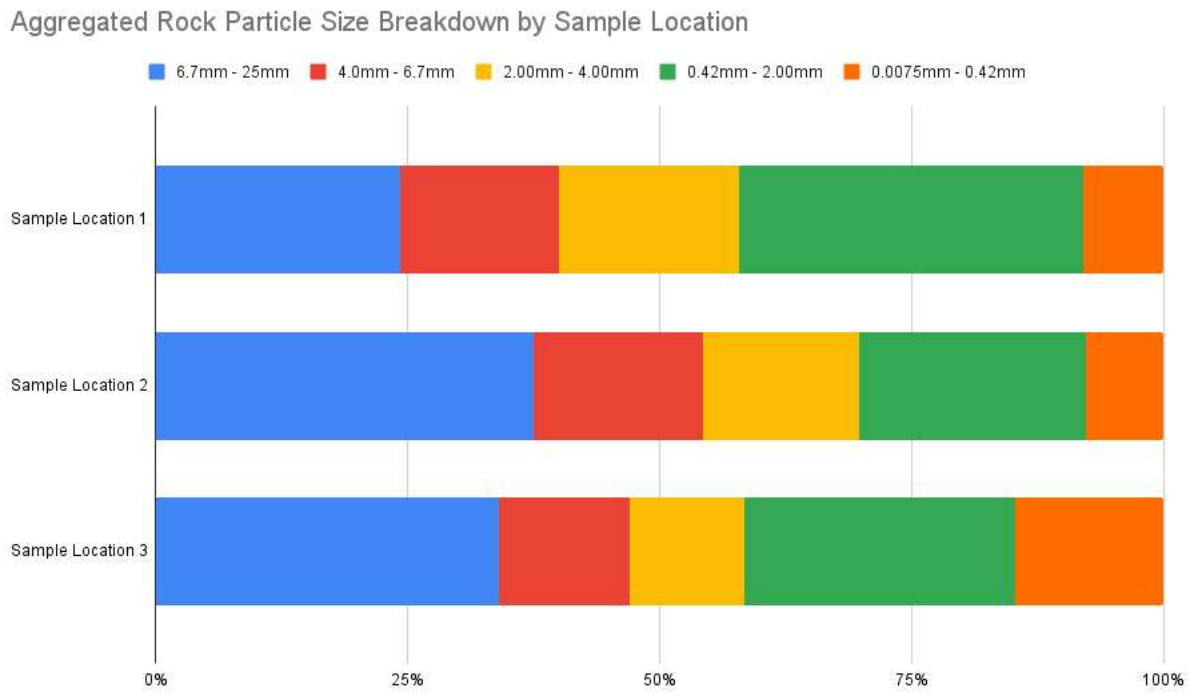

Figure 10 Rock particle distribution analysis results (aggregated)

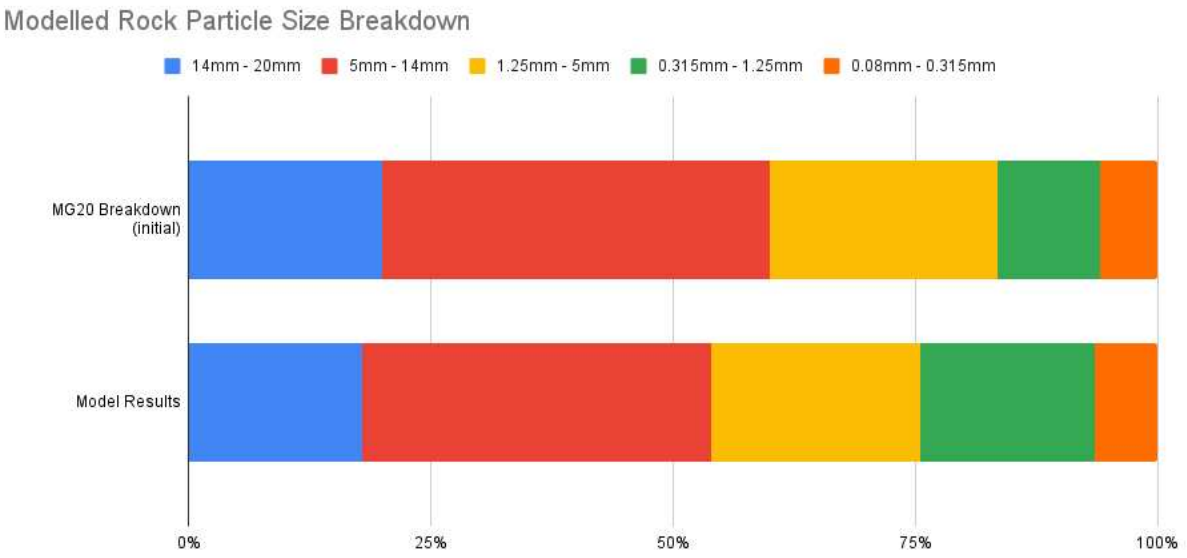

Figure 11 Modelled rock particle breakdown results (initial and after two-year simulation)

Samples from location 1 were found to have the largest amount of size 0.42mm-2.00mm rock particles, with the largest portion of this material found on the road edge. This finding corresponds with the modeled accumulation of smaller particles. The accumulation of these particles along the road's edge may be explained by the crown of the road's surface as described in construction guidelines (B.C. Ministry of Transportation 2007; Skorseth, Ried, and Heiberger 2015).

While a direct comparison between the modeled size breakdown and the result of the sieving analysis is not possible due to mismatching sieve gradations, of note is the disparity between the largest quantity of material by weight. The modeled results predict that most particles should be in the 5mm – 14mm range, while as mentioned, the analysis results show the majority to be in the 0.42mm-2.00mm. This could indicate that the car passage is higher than assumed, and that breakdown available surface area may increase faster than modeled.

Surprisingly, the newest material from location 3 had the most material in the fines 0.42mm to 0.0075mm range. This location was the only location where rock coming from a riverbed was applied to the road surface, which may account for this unexpected result. An interesting comparison that can be loosely made is that of the small particles present between sample locations and from modeled results. The findings from the sample locations indicate that the fines are much more present, with an average of 10.1% of particles less than 0.42mm in the sample locations when compared to the 5.3% of particles less than 0.315mm found in the modeled results.

Location 2 and 3 being of the same age, but from different rock sources present an interesting opportunity to compare distribution changes from similarly aged material. In both cases, the material was applied approximately one year before collection by the same professionals and are geographically within 500m of each other allowing differences in application technique and geographical differences to be eliminated as interfering factors. Despite both materials also passing the MG20 standard for construction, significant differences emerge between the results. Location 2 was found to have a larger proportion of larger-sized particles with nearly 55% of particles over 4mm in size compared to 47% in location 3. Location 2 additionally had a 4% greater number of particles in the 2mm to 4mm range.

Weathering analysis

The results of the weathering analysis resulted in increases in alkalinity for all sample specimens. Sample location 1 had an average increase in alkalinity of 18.33 ppm, while location

2 had an average increase in alkalinity of 19 ppm. Sample location 3 had the highest average increase in alkalinity of 29.3 ppm. The control sample saw no significant increase in alkalinity.

A complication deriving weathering rates from this analysis is that in real-world applications, the material is not fully saturated and may only experience saturation during precipitation events. To correct the weathering rates obtained during the weathering analysis, the time the road material is saturated annually needs to be determined. To this end, the average total rainfall for West Brome based on data from 1971-2000 was determined to be 1.205m (ClimateData.ca, n.d.). It is worth noting that climate modeling predicts higher rainfalls in this area over the next century, under different climate change scenarios (ClimateData.ca, n.d.).

Once the annual rainfall is known, the hydraulic conductivity of the roadway was calculated to be 0,0000417m/s using the Kozeny-Carman equation.

$$K = \frac{g}{v}(8.3x10^{-3})\frac{n^3}{(1-n)^2}d_{10}^2$$

The porosity (n) will be assumed as 0.4, the kinematic viscosity will be that of water at 10C (1,3074 mm^2/s), and the grain diameter for which 10% of the material falls beneath will be 0.075mm, as approximated from the average of material passing from the rock particle distribution analysis leading to the following equation

$$K = \frac{9.8m/s}{1.3074\text{e}-6\text{mm/s}}(8.3x10^{-3})\frac{0.4^3}{(1-0.4)^2}0{,}000075m = 0.0000417m/s$$

With the kinematic viscosity established, and the annual rainfall known, Darcy's Law for vertical flows can be employed, solving for the time that the roadway is saturated, taken to be the time it would take for the rainfall to pass through the roadway:

$$K = \frac{VL}{At\,\Delta h} \rightarrow t = \frac{VL}{AK\,\Delta h} = \frac{1.2m^3 * 0.25m}{(8m * 0.25m) * 0{,}0000348m/s * 0.25m}$$

The time determined that the roadway would be fully saturated annually is 4.79hrs which can then be used in conjunction with the weathering rates obtained during analysis to determine annual weathering rates for the sample locations. The average weathering rates determined during analysis were $2.85\text{x}10^{-7}$ mol/m^2-hr, $4.70\text{x}10^{-7}$ mol/m^2-hr, and $8.58\text{x}10^{-7}$ mol/m^2-hr for locations 1, 2 and 3 respectively. Factoring in the number of hours the roadway is saturated annually, these rates become $1.36\text{x}10^{-6}$ mol/m^2, $2.25\text{x}10^{6}$ mol/m^2, and $4.11\text{x}10^{-6}$ mol/m^2, again for locations 1, 2, and 3 respectively. Surprisingly, location 3 was found to have the highest weathering rate among locations, despite the material being from a riverbed.

While I only considered the time the roadway was saturated as the duration weathering could occur, this is likely an underestimation of the annual weathering. Given that rain events occur frequently throughout the year, there are periods of time where the roadway is partially saturated, and weathering is occurring at a rate proportional to the percentage of roadway that is wet. Knowing this to be the case, we can establish a high estimate of the weathering rate by increasing the time factor from 4.79 hours to 20 hours. This would represent an hour of weathering occurring at near saturated rate for a conservative estimate of 15 annual rainfall events. Using this as the annual time factor for which weathering could occur, our weathering

rates increase to 5.70×10^{-6} mol/m^2, 9.39×10^{-6} mol/m^2, and 1.72×10^{-5} mol/m^2 for locations 1, 2 and 3 respectively.

Once properly converted and input into the model, the results are similar to the results from modeling obtained using a reference value. With the aim of understanding what level of influence maintenance events had on the total amount of carbon transformation when using real-world rates established through my study, I initially ran my model excluding any maintenance events. In this no-maintenance event scenario, the total amount of carbon dioxide transformed over a ten-year period using the rates from the analysis was 186.52 kg, 308.59 kg, and 563.69 kg for locations 1, 2, and 3 respectively, as shown in the figure below.

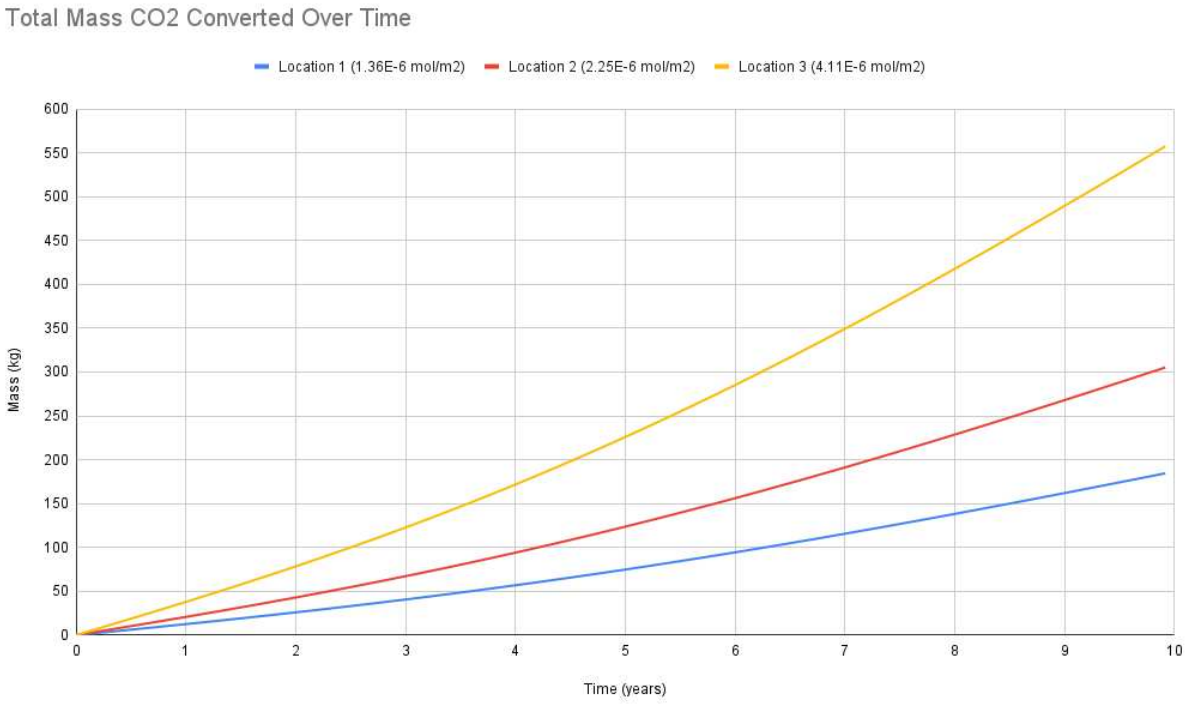

Figure 12 – Modelled total mass of CO2 converted over a ten-year period using weathering rates from analysis

As the results demonstrate, the material used for roadway construction has a definite impact on the potential for carbon dioxide transformation, due to the variability in material weathering rates (even among aggregates). Furthermore, as there is a dependency on rainfall as shown in the rate calculation, meaning that increased precipitation will significantly influence the amount of carbon dioxide transformed. Car passage was thought to be an influential factor on the amount of carbon dioxide transformed, as variability in car passage frequency increases the number of fines. As the roadway materials fractures and becomes smaller, the surface area increases relative to the previous size. Doubling the car passage rate without any maintenance events in the study area found that the contribution to weathering decreased slightly to 151.39 kg, 250.46 kg, and 457.5 kg over the same 10-year period for locations 1, 2 and 3 respectively. Without the addition of new material from maintenance, the rates slowed approaching the ten-year mark, as the available surface area for weathering decreased much more rapidly with the increase in car passage. Within the model, the material lost as dust is a considered to contribute to weathering, however it is a function of car passage while the rock sizing breakdown and material available is considered to be a finite store that decreases to depletion without the addition of new material. This indicates that there is likely a balance point between car passage and maintenance frequency, and that simply increasing car passage without adjusting maintenance frequency will reduce the weathering contribution of a roadway.

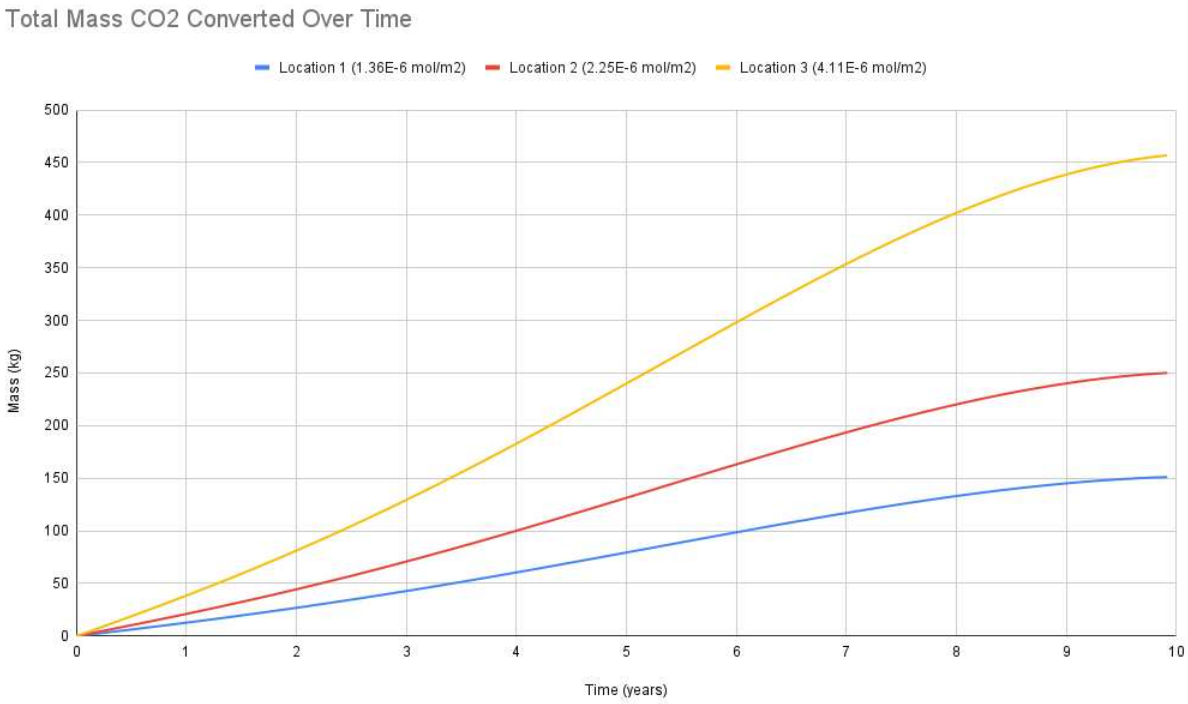

Figure 13 Modelled total mass of CO2 converted over a ten-year period using weathering rates from analysis and doubling car passage rate

To overcome the limiting factor of new material addition, a five-year maintenance cycle was modeled, along with the doubling of the rate of annual daily car passage. The results from this modeling demonstrate another significant increase in the amount of atmospheric carbon dioxide transformed, with total carbon dioxide conversion totaling 293.99 kg, 486.38 kg and 888.45 kg over a 10-year period for locations 1, 2 and 3 respectively, as shown in the following figure.

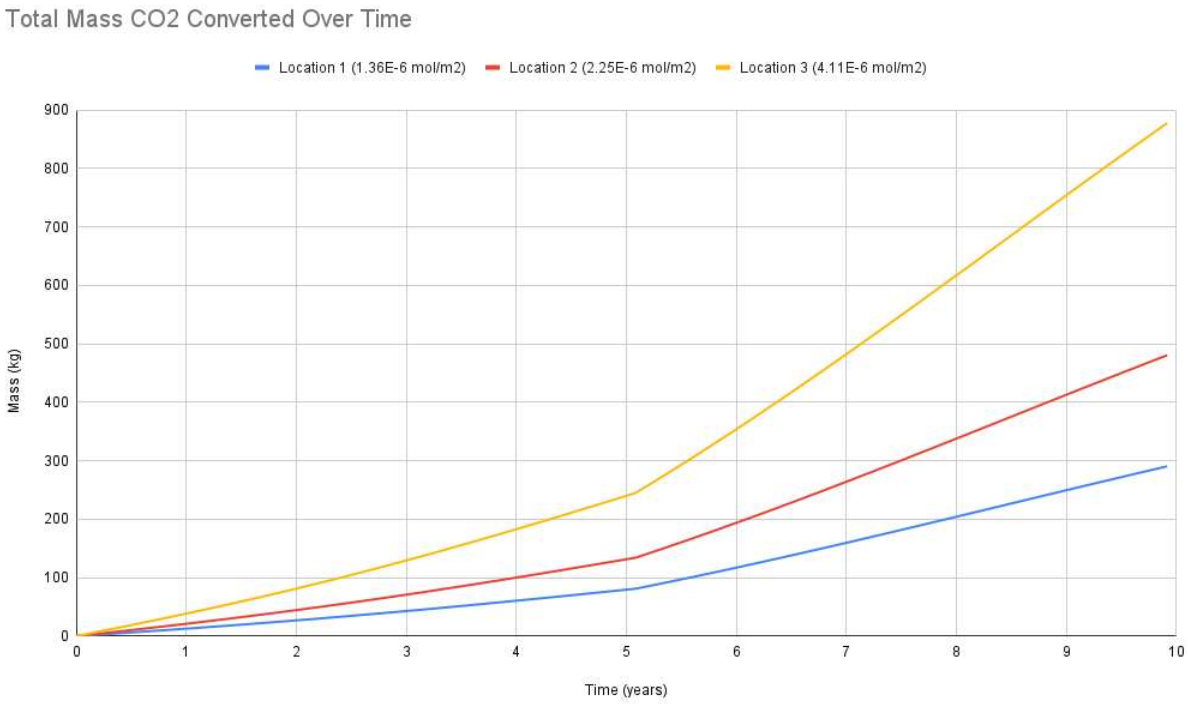

Figure 14 Modelled total mass of CO2 converted over a ten-year period using weathering rates from analysis, doubling car passage rate with a 5-year maintenance frequency

Using the rates from the high estimate, which assumed that weathering occurs at the same rate for an hour after a rainfall event, we can run this simulation again with a five-year maintenance interval and 400 daily car passage results. This simulation yields totals of carbon dioxide transformation of 1232.15kg, 2029.81kg, 3718.08kg for locations 1, 2 and 3 respectively. These results demonstrate a significant increase in the amount of carbon dioxide converted

Chapter 5 – Discussion

Comparison to Other Applications

The results I obtained through weathering analysis are significantly lower than carbon transformation rates found in agricultural applications, and in applications where the purpose is carbon dioxide transformation through rock weathering. That being the case, it is perhaps not a fair comparison to be drawn, as both applications are designed with an objective to remove atmospheric carbon dioxide, while rock weathering is in opposition to goals of roadway construction.

When converted to a rate per area per year, the rates I obtained through weathering analysis become 2.59×10^{-6} kg/m^2/year, 4.29×10^{-6} kg/m^2/year, and 7.83×10^{-6} kg/m^2/year for locations 1, 2 and 3 respectively. Comparing this to a recent quantification in acidic soils which produced a rate of 0.0243 kg/m^2/year, my obtained rates are three orders of magnitude smaller (Dietzen and Rosing 2023).

Despite the Dietzen and Rosing study was situated in geographically similar Greenland, the application was of rock flour to an acidic sandy soil, which is significantly more favourable conditions for rock weathering than used in my research. Sandy soil presents a much less porous medium than gravel allowing for weatherable material to spend significantly more time in contact with rainwater, which I found to be a limiting factor in my research. The particle size used was described to have a median size of 0.0026 mm, which is significantly smaller than my modelled fines with a size 0.080mm allowed for significantly more surface area to be available for weathering (Dietzen and Rosing 2023). Lastly, the soil in the location used by Dietzen and

Rosing had an advantage of being already acidic due to organic material present in the soil, which also presents favourable conditions for rock weathering, while the roadways in my study are intentionally meant to be devoid of organic material, as it can hamper roadway integrity.

Organic materials in soil have been shown to significantly increase the amount of CO_2 that can be transformed by an application of weatherable rock material. A study done in Ontario measuring the carbon sequestration from a wollastonite application in farmlands found carbon transformation rates to be between 0.32 t/ha/5 months and 0.4 t/ha/20 weeks (Haque, Santos, and Chiang 2020). Converting my rates to the same periods, we see that my measured rates are once again several orders of magnitude lower (my rates ranged between $1.08x10^{-5}$ t/ha/5 months to $3.26x10^{-5}$ t/ha/5 months and $1.00x10^{-5}$ t/ha/20 weeks to $3.01x10^{-5}$ t/ha/20 weeks). Despite the significant gap, the accelerated weathering caused by interactions with crops is not year-round, and the weathering of the wollastonite (and associated carbon transformation) is likely to slow after the crops have been harvested.

Recent modelling examining how plant matter interaction affects rock weathering in solids found a rate of 2.3 kg CO_2/m^2/year for a one-time application of 16 kg/m^2, which is six orders of magnitude more than my results (Deng et al. 2023). This research found that soil water retention, plant processes, and carbon dioxide concentration had significant impacts on the weathering rate and noted that modelling for unfavourable conditions saw much less carbon transformation.

The potential for carbon transformation in croplands and farming practices is certainly significantly higher than the observed weathering rates in my study. Nonetheless, it is important to note some significant differences in the objectives of both applications. Incorporation of

weatherable minerals in agriculture is often done with the premise of increasing the amount of carbon transformed, and in some cases a co-benefit of fertilization occurs. In roadway construction and maintenance, the main objective is to produce a safe and durable roadway. In many cases, this is not optional but is required either to continue to provide a safe roadway or to connect new settlements to existing road networks. The rock spread as part of roadways construction and maintenance is by design devoid of organic matter, thus reducing the weathering rate, and is largely comprised of particles significantly greater than those used in agricultural applications.

An interesting observation that I made was that the transport, mining, and application cost in an agricultural scenario were notably absent on the research I consulted. As we previously saw, the mining cost has been shown to be negligible for particles below 1mm, and transportations costs need to be quite significant to exceed the carbon uptake over the lifetime of mined weatherable materials (Moosdorf, Renforth, and Hartmann 2014). Nonetheless, keeping transportation costs to a minimum would allow for significantly more total carbon to be transformed. I decided to dig a bit deeper and found that the total distance between the main source of wollastonite and the agricultural application where a transformation rate of 0.32 t CO_2/ha/5 months was observed is approximately 365km (Haque, Santos, and Chiang 2020). In comparison, the source mines for the rock used in roadway construction for the study sites in my study were 9.4km and 22.3km (as mentioned, two sites share the same quarry, but come from different sections of the quarry). While this difference is significant, further analysis beyond the scope of this study would be needed to obtain total carbon transformation rates, particularly in the areas of carbon production as part of the enhanced rock weathering application.

Significance of Results

This study, to my knowledge, represents the first time that gravel roads as a form of enhanced rock weathering has been researched. This research presents a departure from predominant enhanced rock weathering research pathway of incorporating rock into biotic systems (agriculture or forests) or direct in-situ measurements of background rock weathering without enhancement. While the measured results do not indicate that gravel roadways in the study area are a significant contributor to carbon transformation and atmospheric carbon reduction at small scales, the global impact could be worthy of consideration. As we have seen, factors such as annual precipitation, car passage, and maintenance frequency greatly affect the amount of atmospheric carbon dioxide that can be converted. Knowing that my study area represents only approximately 0.001% of global unpaved roads, gravel roads at a global scale may still be a factor worthy of consideration in the global carbon budget.

Scaling up the lowest annual conversion from the lowest observed rate ($1.36x10^{-6}$ mol/m^2 – annual conversion of 18.65kg) and applying to the global distance of unpaved roads (7 million), we see the potential being (with extreme uncertainty) approximately 14.507 kilotons over 10 years (CIA 2017). Re-doing this simulation using the rate from the high estimate yields a potential of 183.48 kilotons over 10 years. This approximation is quite uncertain, as the definition of unpaved is ambiguous and could refer to dirt roads. Furthermore, the roadway material, road construction techniques, climate, emissions generated from roadway construction and maintenance, and road use vary dramatically at a global scale. While gravel roadways may present an exciting candidate as a contributor to the global carbon research, substantial further research must be performed to improve accuracy of any calculations.

The methodologies used were deliberately "low-tech" – no x-ray spectroscopy, or complex chemical analysis, rather I used instruments that would be accessibly obtained in most cities, if not via online stores. This was done to contribute towards making this research replicable for any unpaved roadway by roadway managers, which was one of my secondary goals. It is my hope that analysing the potential for carbon transformation and selecting a material that allows for a suitable compromise between roadway stability/longevity and carbon transformation could be incorporated into governmental maintenance strategies. Such incorporation could help to remove atmospheric carbon at the same time as improving our understanding of how this form of enhanced weathering contributes to carbon budgets at various scales.

Comparing my obtained rates to reference field rates observed at a similar latitude at Plastic Lake, Ontario of 5.00×10^{-5} mol/m^2, 6.29×10^{-7} mol/m^{2,} and 1.58×10^{-5} mol/m^2 for non-gravel minerals oligoclase, oligoclase, and hornblende respectively are within an order of magnitude higher and lower from the rates I observed (White and Brantley 2003). This indicates that the contribution of gravel roads is within the range of background weathering rates for exposed rock at similar latitudes.

While my results don't point to gravel road construction and maintenance being the significant climate change mitigator I had originally hoped this practice to be, the precipitation influence and roadway factors of car passage and material addition through maintenance likely have significant variability globally. With gravel roads being so ubiquitously distributed globally, the roadways in areas where precipitation is plentiful would have more carbon transformation occurring, particularly when they are high use and high maintenance.

Chapter 6 – Conclusion and Future Direction

Conclusion

The observed rates of weathering during the weathering analysis were close to reference background weathering rates, leading to the overall answer to the research being that gravel roads do indeed contribute to atmospheric carbon dioxide transformation, however, there are limiting factors. The most significant factors influencing the rate of weathering on gravel roadways that emerged were the annual amount of rainfall in the geographical location, the maintenance frequency (addition of new material), and the mechanical fracturing of the road material due to car passage. Surprisingly, the material quarried from a riverbed at location 3 had the most amount of fine material, despite being one of the two applications with an age of one year at the time of analysis. As anticipated, the oldest sample from location 1 had the slowest weathering rate, supporting previous research finding a decrease in weathering potential over time.

The modeling results using the rates observed derived from the weathering analysis show a limited amount of contribution to the reduction of atmospheric carbon dioxide at small scales, however the combination of the addition of new material through maintenance events and mechanical fracturing of the rock material due to car passage along with maintenance frequency showed great influence on this result. Despite the limited contribution, the global contribution of this unintentional weathering practice could be quite significant. This study suggests that further research into the subject would be merited to better understand the global impact of gravel roadway construction and maintenance as a carbon reduction strategy.

As the difference in rates between location 2 (ground quarried rock) and location 3 (riverbed quarried rock) demonstrates, the material source can have a significant effect on the transformation of atmospheric carbon dioxide through weathering. A potential explanation for this discrepancy could be the length of time the quarried rock is stored before roadway application. It is unlikely that freshly quarried rock is applied immediately to roadways, and weathering of the rock material could occur before application during storage.

The model produced has proven to be of great use, resulting in similar outcomes when using theoretical values and when using real-world values. Should it be sought to be used for roadway management, it can be relatively easily used to determine the impacts of the rock material, annual daily car passage rate, and maintenance rate on the transformation of atmospheric carbon dioxide through weathering.

Limitations

A noteworthy limitation of the results is the lack of accurate car passage data for sample locations. Estimates were used during modeling, and as it has been shown, annual daily car passage has a strong influence on the amount of transformed atmospheric carbon dioxide through weathering. Furthermore, the initial distribution of material used on the roadway application was not verified at the time of application, as the material distribution certification occurs annually to certify the material in storage at the quarry. Further to this, the porosity of the roadway surface was estimated for modeling, potentially influencing the volume and ultimately surface area available for weathering. Lastly, materials lost as dust were modeled to have just below the diameter of the smallest increment of material: 0.079mm.

During the weathering analysis, there was some temperature variability of the samples, potentially affecting the weathering reactions. Temperatures ranged from 22.9C to 28.8C throughout the analysis, high enough for reaction to occur, but potentially influencing the reaction rate. Alkalinity as $CaCO_3$ was the only measurement taken as a proxy for calcite weathering, however, it is possible other weathering reactions occurred that were not measured. The effect of unmeasured weathering reactions could lead to the weathering rates found being lower than a weathering rate that considers all rock weathering reactions occurring.

Future Directions

This research explores an existing anthropogenic practice of unintentional enhanced rock weathering and produces a model that can be used to inform on climate change effects when managing roadways. As previously seen, much of the research on enhanced rock weathering is limited to the field of agriculture, so it is hoped that this research broadens the minds of readers to explore the modification of existing practices to incorporate negative emissions strategies. Furthermore, it is my hope that this research allows for gravel road construction and maintenance to be considered as a carbon reduction technology, even if the enhanced weathering from this practice is unintentional.

Should this work be expanded upon, a direction could be to investigate the weathering rates of rock material from quarrying to roadways, and for a period after application onto roadways to improve the accuracy of the contribution of gravel roadway construction and maintenance on the transformation of atmospheric carbon dioxide. Additional to this would be the calculation of the emissions required to quarry and apply the rock to the roadway, to obtain a

more holistic understanding of the contribution of gravel roadway construction and maintenance as a negative emissions strategy.

Another expansion of the research would be the refinement of the weathering rate. The equipment used to determine the weathering rate was sufficient for this study, however, better equipment exists to determine the multiple types of weathering that could occur on gravel road material. Given that roadway material is often sourced locally, the development of a reliable and accessible method to determine all the types of carbon-transforming weathering would not only improve the accuracy of the weathering rates found within this study but reduce barriers to the incorporation of the impacts on atmospheric carbon dioxide as a factor of roadway management.

The model produced could be improved upon to include rainfall as a variable, allowing the model to be used in a wide range of climates. Furthermore, functionality to better account for the material lost as dust through weathering could improve the accuracy of the modeled results, as this presents a significant surface area that can interact with the surrounding vegetation to weather at an accelerated rate. While an ambitious undertaking, the model could be translated into an open-sourced language such as Python or Julia to further remove accessibility barriers.

Lastly, the impact of snowfall and freeze-thaw cycles was not accounted for in modeling or the determination of weathering rates. Freeze-thaw cycles could further impact the fracturing of roadway material leading to an even more rapid increase of surface area available for weathering. Snowfall could also increase the time that the roadway remains saturated, leading to a higher weathering rate from a longer reaction time. Should research into this be performed, incorporation of the results could be added to the model to further improve its accuracy.

References

Alberta Transportation. 2000. “Highway Maintenance Guidelines and Level of Service Manual.” https://open.alberta.ca/dataset/84604631-aec2-4a7d-98f3-060ad2ff6fe8/resource/80f63d44-388b-4924-b2a6-d61705fca62c/download/2000-highway-maintenance-guidelines-level-service-manual-2000-06-14.pdf.

B.C. Ministry of Transportation. 2007. “500 - Low Volume Roads Chapter.” In *B.C. Supplement to TAC Geometric Design Guide for Canadian Roads*, 500i-500.13. BC Ministry of Transportation. https://www2.gov.bc.ca/assets/gov/driving-and-transportation/transportation-infrastructure/engineering-standards-and-guidelines/highway-design-and-survey/tac/tools/low_volume_roads-interim_guidelines.pdf.

Beerling, David J., Euripides P. Kantzas, Mark R. Lomas, Peter Wade, Rafael M. Eufrasio, Phil Renforth, Binoy Sarkar, et al. 2020. “Potential for Large-Scale CO2 Removal via Enhanced Rock Weathering with Croplands.” *Nature 2020 583:7815* 583 (7815): 242–48. https://doi.org/10.1038/S41586-020-2448-9.

Berner, Robert A. 1978. “Rate Control of Mineral Dissolutions under Earth Surface Conditions.” *American Journal of Science* 278:1235–52. http://www.ajsonline.org/content/278/9/1235.full.pdf.

Berthelot, Curtis, and Allan Carpentier. 2007. “Gravel Loss Characterization and Innovative Preservation Treatments of Gravel Roads: Saskatchewan, Canada.” *Transportation*

Research Record: Journal of the Transportation Research Board 1819 (1): 180–84. https://doi.org/10.3141/1819b-23.

Bray, Andrew W, Eric H Oelkers, Steeve Bonneville, Domenik Wolff-Boenisch, Nicola J Potts, Gary Fones, and Liane G Benning. 2015. "The Effect of PH, Grain Size, and Organic Ligands on Biotite Weathering Rates." *Geochimica et Cosmochimica Acta* 164 (August):127–45. https://doi.org/10.1016/J.GCA.2015.04.048.

CIA. 2017. *The World Factbook*. 2016th–2017th ed. Central Intelligence Agency. https://doi.org/10.1016/j.petrol.2013.05.007.

ClimateData.ca. n.d. "West Brome QC ClimateData.Ca." ClimateData.Ca. Accessed August 13, 2024. https://climatedata.ca/explore/location/?loc=EKOAU&location-select-temperature=tx_max&location-select-precipitation=r1mm&location-select-other=frost_days&dataset_name=cmip5.

Colman, Steven M. 1981. "Rock-Weathering Rates as Functions of Time." *Quaternary Research* 15 (3): 250–26445. https://doi.org/10.1016/0033-5894(81)90029-6.

Deng, Hang, Eric Sonnenthal, Bhavna Arora, Hanna Breunig, Eoin Brodie, Markus Kleber, Nicolas Spycher, and Peter Nico. 2023. "The Environmental Controls on Efficiency of Enhanced Rock Weathering in Soils." *Scientific Reports 2023 13:1* 13 (1): 1–10. https://doi.org/10.1038/S41598-023-36113-4.

Dietzen, Christiana, Robert Harrison, and Stephani Michelsen-Correa. 2018. "Effectiveness of Enhanced Mineral Weathering as a Carbon Sequestration Tool and Alternative to

Agricultural Lime: An Incubation Experiment." *International Journal of Greenhouse Gas Control* 74 (August):251–58. https://doi.org/10.1016/j.ijggc.2018.05.007.

Dietzen, Christiana, and Minik T. Rosing. 2023. "Quantification of CO2 Uptake by Enhanced Weathering of Silicate Minerals Applied to Acidic Soils." *International Journal of Greenhouse Gas Control* 125 (May):103872. https://doi.org/10.1016/J.IJGGC.2023.103872.

DMTI Spatial Inc. 2018. "DMTI CanMap Route Logistics." Markham: DMTI Spatial Inc.

Earle, Steven. 2015. *Physical Geology*. *Physical Geology*. BCcampus. https://opentextbc.ca/geology/chapter/5-2-chemical-weathering/.

Edwards, David P, Felix Lim, Rachael H James, Christopher R Pearce, Julie Scholes, Robert P Freckleton, and David J Beerling. 2017a. "Climate Change Mitigation: Potential Benefits and Pitfalls of Enhanced Rock Weathering in Tropical Agriculture." *Biology Letters* 13 (4). https://doi.org/10.1098/rsbl.2016.0715.

Edwards, David P., Felix Lim, Rachael H. James, Christopher R. Pearce, Julie Scholes, Robert P. Freckleton, and David J. Beerling. 2017b. "Climate Change Mitigation: Potential Benefits and Pitfalls of Enhanced Rock Weathering in Tropical Agriculture." *Biology Letters* 13 (4). https://doi.org/10.1098/RSBL.2016.0715.

"Emission Facts: Average Carbon Dioxide Emissions Resulting from Gasoline and Diesel Fuel (EPA420-F-05-001)." 2005. www.epa.gov/otaq/greenhousegases.htm.

Frings, Roy M, Holger Schüttrumpf, and Stefan Vollmer. 2011. "Verification of Porosity Predictors for Fluvial Sand-Gravel Deposits." *Water Resources Research* 47 (7). https://doi.org/10.1029/2010WR009690.

Hallet, Bernard. 2006. “Why Do Freezing Rocks Break ?” *Science* 314 (5802): 1092–93. https://doi.org/10.1126/science.1135200.

Haque, Fatima, Rafael M. Santos, and Yi Wai Chiang. 2020. “CO2 Sequestration by Wollastonite-Amended Agricultural Soils – An Ontario Field Study.” *International Journal of Greenhouse Gas Control* 97 (June):103017. https://doi.org/10.1016/J.IJGGC.2020.103017.

Heberlein, Thomas A. 2013. *Navigating Environmental Attitudes*. *Navigating Environmental Attitudes*. Oxford University Press. https://doi.org/10.1093/acprof:oso/9780199773329.001.0001.

Israeli, Yoni, and Simon Emmanuel. 2018. “Impact of Grain Size and Rock Composition on Simulated Rock Weathering.” *Earth Surface Dynamics* 6 (2): 319–27. https://doi.org/10.5194/esurf-6-319-2018.

Jiang, Hao, Wenjing Liu, Zhifang Xu, Xiaode Zhou, Ziyan Zheng, Tong Zhao, Li Zhou, Xuan Zhang, Yifu Xu, and Taoze Liu. 2018. “Chemical Weathering of Small Catchments on the Southeastern Tibetan Plateau I: Water Sources, Solute Sources and Weathering Rates.” *Chemical Geology* 500 (August):159–74. https://doi.org/10.1016/j.chemgeo.2018.09.030.

Kantola, Ilsa B, Michael D Masters, David J Beerling, Stephen P Long, and Evan H DeLucia. 2017. “Potential of Global Croplands and Bioenergy Crops for Climate Change Mitigation through Deployment for Enhanced Weathering.” *Biology Letters*. https://doi.org/10.1098/rsbl.2016.0714.

Kantzas, Euripides P., Maria Val Martin, Mark R. Lomas, Rafael M. Eufrasio, Phil Renforth, Amy L. Lewis, Lyla L. Taylor, et al. 2022. "Substantial Carbon Drawdown Potential from Enhanced Rock Weathering in the United Kingdom." *Nature Geoscience 2022 15:5* 15 (5): 382–89. https://doi.org/10.1038/S41561-022-00925-2.

Kasting, J F. 1984. "Comments on the BLAG Model: The Carbonate-Silicate Geochemical Cycle and Its Effect on Atmospheric Carbon Dioxide over the Past 100 Million Years." *American Journal of Science* 284 (10): 1175–82. https://doi.org/10.2475/ajs.284.10.1175.

Kennebec County Soil and Water Conservation District, and Maine Department of Environmental Protection Bureaus of Land Resources and Water Quality. 2016. *Gravel Road Maintenance Manual: A Guide for Landowners on Camp and Other Gravel Roads*. https://www.maine.gov/dep/land/watershed/camp/road/gravel_road_manual.pdf.

Kump, Lee R, Susan L Brantley, and Michael A Arthur. 2000. "Chemical Weathering, Atmospheric CO 2 , and Climate." *Annual Review of Earth and Planetary Sciences* 28 (1): 611–67. https://doi.org/10.1146/annurev.earth.28.1.611.

Larkin, Christina S., M. Grace Andrews, Christopher R. Pearce, Kok L. Yeong, David J. Beerling, Joshua Bellamy, Suzan Benedick, et al. 2022. "Quantification of CO2 Removal in a Large-Scale Enhanced Weathering Field Trial on an Oil Palm Plantation in Sabah, Malaysia." *Frontiers in Climate* 4 (August):959229. https://doi.org/10.3389/FCLIM.2022.959229/BIBTEX.

Lawford-Smith, H, and A Currie. 2017. "Accelerating the Carbon Cycle: The Ethics of Enhanced Weathering." *Biology Letters* 13 (4). https://doi.org/10.1098/rsbl.2016.0859.

Lehmann, Nele, Hugues Lantuit, Michael Ernst Böttcher, Jens Hartmann, Antje Eulenburg, and Helmuth Thomas. 2023. “Alkalinity Generation from Carbonate Weathering in a Silicate-Dominated Headwater Catchment at Iskorasfjellet, Northern Norway.” *Biogeosciences* 20 (16): 3459–79. https://doi.org/10.5194/BG-20-3459-2023.

May, Matthias M, and Kira Rehfeld. 2019. “ESD Ideas: Photoelectrochemical Carbon Removal as Negative Emission Technology.” *Earth System Dynamics* 10 (1): 1–7. https://doi.org/10.5194/esd-10-1-2019.

McDonald, Tom, and Bob Sperry. 2014. “Highway Maintenance and Operations Handbook.” http://www.dot.state.ak.us/stwddes/research/assets/pdf/ak_maint-ops_hb.pdf.

Millot, Romain, Jérôme Gaillardet, Bernard Dupré, and Claude Jean Allègre. 2002. “The Global Control of Silicate Weathering Rates and the Coupling with Physical Erosion: New Insights from Rivers of the Canadian Shield.” *Earth and Planetary Science Letters* 196 (1–2): 83–98. https://doi.org/10.1016/S0012-821X(01)00599-4.

Monlux, Stephen, Michael Mitchell, and S Monlux. 1989. “Chloride Stabilization of Unpaved Road Aggregate Surfacing.” *Transportation Research Record: Journal of the Transportation Research Board* 2:50–58. https://doi.org/10.3141/1989-48.

Montserrat, Francesc, Phil Renforth, Jens Hartmann, Martine Leermakers, Pol Knops, and Filip J R Meysman. 2017. “Olivine Dissolution in Seawater: Implications for CO2 Sequestration through Enhanced Weathering in Coastal Environments.” *Environmental Science and Technology* 51 (7): 3960–72. https://doi.org/10.1021/acs.est.6b05942.

Moosdorf, Nils, Phil Renforth, and Jens Hartmann. 2014. “Carbon Dioxide Efficiency of Terrestrial Enhanced Weathering.” *Environmental Science and Technology* 48 (9): 4809–16. https://doi.org/10.1021/es4052022.

Naimi, Babak, and Alexey Voinov. 2012. “StellaR: A Software to Translate Stella Models into R Open-Source Environment.” *Environmental Modelling & Software* 38 (December):117–18. https://doi.org/10.1016/J.ENVSOFT.2012.05.012.

National Oceanic and Atmospheric Administration. 2022. “Carbon Dioxide Now More than 50% Higher than Pre-Industrial Levels.” June 3, 2022. https://www.noaa.gov/news-release/carbon-dioxide-now-more-than-50-higher-than-pre-industrial-levels.

Pidgeon, Nick F, and Elspeth Spence. 2017. “Perceptions of Enhanced Weathering as a Biological Negative Emissions Option.” *Biology Letters* 13 (4). https://doi.org/10.1098/rsbl.2017.0024.

Rastegari Mehr, Meisam, Behnam Keshavarzi, and Armin Sorooshian. 2019. “Influence of Natural and Urban Emissions on Rainwater Chemistry at a Southwestern Iran Coastal Site.” *Science of The Total Environment* 668 (June):1213–21. https://doi.org/10.1016/J.SCITOTENV.2019.03.082.

Schuiling, R D, and P Krijgsman. 2006. “Enhanced Weathering: An Effective and Cheap Tool to Sequester CO 2.” *Climatic Change* 74 (1–3): 349–54. https://doi.org/10.1007/s10584-005-3485-y.

Schuiling, Roelof Dirk. 2017. “Olivine Weathering against Climate Change.” *Natural Science* 09 (01): 21–26. https://doi.org/10.4236/ns.2017.91002.

Skorseth, Ken, Richard Ried, and Katherine Heiberger. 2015. *Gravel Roads Maintenance and Design Manual*. 2nd ed. Federal Highway Administration (FHWA) and the South Dakota Local Technical Assistance Program (SDLTAP).

Skorseth, Ken, and Ali A Selim. 2000. "Section III: Surface Gravel." In *Gravel Roads: Maintenance and Design Manual*, 39–50. US Department of Transportation. https://www.epa.gov/sites/production/files/2015-10/documents/2003_07_24_nps_gravelroads_sec3_0.pdf.

Smith, S M, O Geden, M J Gidden, W F Lamb, G F Nemet, J C Minx, H Buck, et al. 2024. "The State of Carbon Dioxide Removal - 2nd Edition." The State of Carbon Dioxide Removal. https://osf.io/f85qj/.

Statistics Canada. 2009. "Envirostats." Statistics Canada. https://www150.statcan.gc.ca/n1/pub/16-002-x/16-002-x2009001-eng.pdf.

Strefler, Jessica, Thorben Amann, Nico Bauer, Elmar Kriegler, and Jens Hartmann. 2018. "Potential and Costs of Carbon Dioxide Removal by Enhanced Weathering of Rocks." *Environmental Research Letters* 13 (3): 34010. https://doi.org/10.1088/1748-9326/aaa9c4.

Taksavasu, Tadsuda, Piyanat Arin, Thanakon Khatecha, and Suchanya Kojinok. 2024. "Microtextural Characteristics of Ultramafic Rock-Forming Minerals and Their Effects on Carbon Sequestration." *Minerals* 14 (6): 597. https://doi.org/10.3390/MIN14060597/S1.

Taylor, Lyla L, Joe Quirk, Rachel M S Thorley, Pushker A Kharecha, James Hansen, Andy Ridgwell, Mark R Lomas, Steve A Banwart, and David J Beerling. 2016. "Enhanced

Weathering Strategies for Stabilizing Climate and Averting Ocean Acidification." *Nature Climate Change* 6 (4): 402–6. https://doi.org/10.1038/nclimate2882.

The Pennsylvania State University. 2018. *Driving Surface Aggregate (DSA) Handbook*. Penn State University. https://www.dirtandgravel.psu.edu/sites/default/files/General.

White, Art F, and Susan L Brantley. 2003. "The Effect of Time on the Weathering of Silicate Minerals: Why Do Weathering Rates Differ in the Laboratory and Field?" *Chemical Geology* 202 (3–4): 479–506. https://doi.org/10.1016/j.chemgeo.2003.03.001.

Tables

Sample	Location	Initial (g)	Bag (g)	26.5mm	Percent Passing 26.5mm	6.7mm	Percent Passing 6.7mm	4.00mm	Percent Passing 4.00mm	2.00mm	Percent Passing 2.00mm	0.42mm	Percent Passing 0.42mm	0.0075mm	Percent Passing 0.0075mm	Less than 0.0075mm	Error in accuracy (g)
1	Road Edge (RE)	1407.7	12.4	0	100	395.7	70.99%	216.7	55.59%	191.2	42.01%	542	3.51%	49.3	0.01%	0.1	0.3
1	Road Center (RC)	1062.5	12.3	0	100	208.3	79.25%	168.9	63.35%	219.5	42.69%	361.6	8.66%	90.3	0.16%	1.7	-0.1
1	Lane Center (LC)	1073	12.4	0	100	231.5	77.18%	139.2	64.20%	200.7	45.50%	339.5	13.86%	145.2	0.33%	3.5	1
2	Road Edge (RE)	1234.4	12	0	100	416	65.29%	181	50.63%	170.3	36.84%	415.7	3.16%	38.9	0.01%	0.1	0.4
2	Road Center (RC)	1104.7	12.1	0	100	252.6	75.86%	207	57.12%	203.9	38.66%	307.7	10.81%	117.2	0.20%	2.2	2
2	Lane Center (LC)	1321.9	12.2	0	100	417.6	67.33%	180.1	53.71%	210.3	37.80%	372.7	9.61%	123.9	0.23%	3.1	2
3	Road Edge (RE)	1207.7	12	0	100	350.6	69.88%	197.8	53.51%	204.6	36.57%	409.1	2.69%	32.3	0.02%	0.2	1.1
3	Road Center (RC)	950.6	12	0	100	101.8	87.62%	170.4	69.69%	197.1	48.96%	317.3	15.58%	146.4	0.18%	1.7	3.9
3	Lane Center (LC)	1018.7	12	0	100	200.3	78.99%	170.1	62.30%	200.8	42.58%	317.8	11.39%	113.7	0.23%	2.3	1.7
4	Road Edge (RE)	1127.3	11.9	0	100	311.6	71.12%	159.8	56.94%	147.8	43.83%	451.6	3.77%	42.4	0.01%	0.1	2.1
4	Road Center (RC)	1273	12.3	0	100	237.2	80.27%	203.4	64.30%	253.6	44.38%	462.3	8.06%	100.5	0.16%	2.1	1.6
4	Lane Center (LC)	1319.1	12	0	100	250	79.49%	214.4	63.23%	277.8	42.17%	442.2	8.65%	111.6	0.19%	2.5	8.6
5	Road Edge (RE)	1447.6	11.8	0	100	410	70.75%	210.9	56.18%	216.7	41.21%	548.6	3.32%	47.6	0.03%	0.4	1.6
5	Road Center (RC)	1241	12.1	0	100	253.3	78.56%	213.2	61.38%	243.9	41.72%	384.9	10.71%	130.6	0.19%	2.3	0.7
5	Lane Center (LC)	1312.7	12	0	100	185.8	84.83%	211.3	68.73%	267	48.39%	530.8	7.95%	102.9	0.11%	1.5	1.4

Table 1 Rock Breakdown Analysis, Location 1

Sample	Location	Initial (g)	Bag (g)	26.5mm	Percent Passing 26.5mm	6.7mm	Percent Passing 6.7mm	4.00mm	Percent Passing 4.00mm	2.00mm	Percent Passing 2.00mm	0.42mm	Percent Passing 0.42mm	0.0075mm	Percent Passing 0.0075mm	Less than 0.0075mm	Error in accuracy (g)
6	Road Edge (RE)	1349.7	12.3	0	100	448.8	65.87%	192.4	51.61%	196.5	37.05%	403.8	7.13%	95.7	0.04%	0.6	-0.4
6	Road Center (RC)	1194.5	12	0	100	352	69.49%	241.4	49.28%	212.7	31.47%	300.6	6.30%	74.9	0.03%	0.4	0.5
6	Lane Center (LC)	1131.8	12.1	0	100	440.5	60.09%	196.9	42.69%	182.4	26.58%	225.2	6.68%	73.5	0.19%	2.1	-0.9
7	Road Edge (RE)	1470.8	24.2	0	100	587.3	58.40%	184.3	45.87%	187.3	33.14%	366.3	8.23%	120.6	0.03%	0.5	0.3
7	Road Center (RC)	1277.9	12	0	100	459.6	63.11%	228.5	45.23%	212.3	28.62%	296.4	5.42%	68.4	0.07%	0.9	-0.2
7	Lane Center (LC)	1358.6	12.1	0	100	451.1	65.87%	245.1	47.83%	235.5	30.49%	312.2	7.52%	100.9	0.09%	1.2	0.5
8	Road Edge (RE)	1172.3	12.3	0	100	430	62.26%	165.2	48.17%	158.9	34.62%	269.7	11.61%	135.4	0.06%	0.7	0.1
8	Road Center (RC)	1118.6	12	0	100	342.1	68.34%	215.8	49.05%	193.6	31.75%	258.8	8.61%	94.7	0.14%	1.6	0
8	Lane Center (LC)	1212.8	12	0	100	490.5	58.74%	196.9	42.50%	179.7	27.69%	251.7	6.93%	83.1	0.08%	1	-2.1
9	Road Edge (RE)	1249.2	12	0	100	354.2	70.68%	241.3	51.36%	225.5	33.31%	311.1	8.41%	104.1	0.07%	0.9	0.1
9	Road Center (RC)	0	12.1	0		450.2		192.9		190.6		325.3		106.9		0	N/A Missed Initial Tare
9	Lane Center (LC)	1204.1	12	0	100	447	62.00%	223.3	43.46%	189.5	27.72%	241.2	7.69%	91.1	0.12%	1.5	-1.5
10	Road Edge (RE)	1203.4	12.4	0	100	590.8	49.83%	140.3	38.17%	114.3	28.67%	166.1	14.87%	131.5	3.94%	47.4	0.6
10	Road Center (RC)	1513.9	12.1	0	100	614.6	58.62%	241.2	42.69%	223.6	27.92%	329.3	6.17%	92.6	0.05%	0.8	-0.3
10	Lane Center (LC)	1432.7	12	0	100	515.2	63.24%	271.5	44.29%	232.8	28.04%	293.8	7.54%	106.7	0.09%	1.3	-0.6

Table 2 Rock Breakdown Analysis, Location 2

Sample	Location	Initial (g)	Bag (g)	26.5mm	Percent Passing 26.5mm	6.7mm	Percent Passing 6.7mm	4.00mm	Percent Passing 4.00mm	2.00mm	Percent Passing 2.00mm	0.42mm	Percent Passing 0.42mm	0.0075mm	Percent Passing 0.0075mm	Less than 0.0075mm	Error in accuracy (g)
11	Road Edge (RE)	1394.7	12.1	0	100	438.6	67.71%	114.8	59.48%	146.7	48.96%	453.3	16.46%	228.7	0.06%	0.9	-0.4
11	Road Center (RC)	936.3	12	0	100	298.7	66.89%	163.1	49.47%	126.4	35.97%	195.4	15.10%	139.2	0.23%	2.2	-0.7
11	Lane Center (LC)	1294	12.2	0	100	466.6	62.97%	175.4	49.41%	139.5	38.63%	287.9	16.38%	203.5	0.66%	8.5	0.4
12	Road Edge (RE)	1210.6	12	0	100	350.8	69.99%	105.9	61.24%	119.6	51.36%	396.4	18.62%	221.4	0.33%	4	0.5
12	Road Center (RC)	859.3	11.9	0	100	285.3	65.41%	139	49.24%	117.3	35.59%	194.6	12.94%	109.3	0.22%	1.9	0
12	Lane Center (LC)	1451.1	12.1	0	100	445.3	68.42%	205	54.30%	169	42.65%	462.7	10.76%	154	0.15%	2.2	0.8
13	Road Edge (RE)	1059.7	12.1	0	100	325.1	68.08%	94.5	59.16%	78.5	51.75%	310.3	22.47%	232.7	0.51%	5.4	1.1
13	Road Center (RC)	1177.2	12.1	0	100	366.3	67.83%	204.3	50.48%	181.9	35.02%	285.4	10.78%	125.8	0.09%	1.1	0.3
13	Lane Center (LC)	1090.3	12.1	0	100	430.7	59.38%	131.9	47.28%	102	37.93%	234.9	16.38%	170.9	0.71%	7.7	0.1
14	Road Edge (RE)	1364.2	12.3	0	100	428.2	67.50%	104	59.88%	105.8	52.13%	290.3	30.85%	393.2	2.02%	27.6	2.8
14	Road Center (RC)	921.9	12	0	100	293.9	66.72%	156.9	49.70%	137.7	34.77%	195.6	13.55%	124.3	0.07%	0.6	0.9
14	Lane Center (LC)	1591.5	12.2	0	100	657	57.89%	190.6	45.91%	157.7	36.00%	389.8	11.51%	178.6	0.29%	4.6	1
15	Road Edge (RE)	1591.7	12.7	0	100	528.8	65.89%	127.9	57.86%	122.8	50.14%	556.8	15.16%	236.9	0.28%	4.4	1.4
15	Road Center (RC)	1730.4	12.2	0	100	497.4	70.39%	333	51.15%	263.8	35.90%	539.6	4.72%	80.8	0.05%	0.9	2.7
15	Lane Center (LC)	1527.2	12.5	0	100	519.3	65.15%	192.2	52.56%	186.2	40.37%	467.1	9.78%	145.4	0.26%	4	0.5

Table 3 Rock Breakdown Analysis, Location 3

Sample	Material Weight	Δ[HCO3-] (mol)	Total Surface Area available	Δ[HCO3-] (mol) per m2	Δ[HCO3-] (mol) per m2 per hour
Site 1 - 1	54.7	9.60E-07	0.0281	3.41E-05	2.85E-07
Site 1 - 2	54.0	1.74E-06	0.0278	6.29E-05	5.24E-07
Site 1 - 3	58.6	1.67E-06	0.3012	5.54E-06	4.62E-08
Site 2 - 1	51.4	1.38E-06	0.1782	7.72E-06	6.43E-08
Site 2 -2	52.8	1.46E-06	0.0183	8.00E-05	6.67E-07
Site 2 - 3	55.8	1.57E-06	0.0193	8.13E-05	6.78E-07
Site 3 - 1	51.4	2.22E-06	0.0207	1.07E-04	8.90E-07
Site 3 - 2	51.6	2.15E-06	0.0208	1.03E-04	8.61E-07
Site 3 - 3	54.0	2.15E-06	0.0218	9.88E-05	8.23E-07

Table 4 Rainwater dependant weathering rates per weathering analysis specimen

Supplementary Data

Béton Optimal Inc.
Optimal Concrete Inc.
www.betonoptimal.com
ison de Groupe ABS Inc

ESSAIS SUR MATÉRIAUX GRANULAIRES

Laboratoire
371 rue Léger
Sherbrooke, Qc

Client: Normand Jeanson Excavation **N° Projet:**

ÉCHANTILLONNAGE	
No Échantillon:	917325
Type de matériaux:	Pierre Concassé
Calibre:	MG20b
Provenance:	Carrière Mine de Stukley
Localisation prélèv:	Réserve en carrière - Échant. n°1
Date :	2018-03-02
Échantilonné par:	François Gagnon

Remarques:
Échantillonnage effectué selon la norme CSA A23.2-1A

GRANULOMÉTRIE
CSA A23.2-2A & 5A / LC 21-040

Tamis	% passant	Exigences	Statut
112 mm	100		C
80 mm	100		C
56 mm	100		C
31.5 mm	100	100	C
20 mm	93	90-100	C
14 mm	76	68-93	C
10 mm	62	s.o	C
5 mm	42	35-60	C
2.5 mm	30	s.o	C
1.25 mm	22	19-38	C
0.630 mm	16	s.o	C
0.315 mm	13	9-17	C
0.160 mm	12	s.o	C
0.080 mm	7,9	5-9	C

AUTRES ESSAIS	RÉSULTAT	EXIGENCE	
Propreté (80um) CSA A23.2-5A	1,58	11	C
Colorimétrie CSA A23.2-7A			
Micro-Deval	12,6	35	C
Grade F LC21-070			
Los Angeles CSA A23.2-16A			
Particules Plates LC 21-265			
Particules Allongées LC 21-265			
Plates & Allongées LC 21-265			
Particules légères CSA A23.2-4A			
Fragmentation LC 21-100			
Gel/dégel non confiné CSA A23.2-24A			
Mottes d'argile & Part. friable (fins) CSA A23.2-3A			
Mottes d'argile & Part. friable (gros) CSa A23.2-3A			
Densité Brute			
Densité SSS			
Densité apparente			
Absorption %			
Valeur au bleu LC 21-255			
Masse Volumique CSA A23.2-10A			
Tassée (Kg/m^3)			
Non-Tassée (Kg/m^3)			
Proctor Modifié BNQ 2501-255		Kg/m^3 W%	
Matière Organique LC 31-228			

Approuvé par: François Gagnon, Tech Sr. Date: 2018-03-08

Supplementary Data 1 MG20 Certification analysis

Time (hrs)	Sample Location	Sample	EC (µS/cm)	TDS (ppm)	Temp (C)	pH	Full Container Weight	Alkalinity (ppm)
0	**1**	**Site 1 - 1**	20	10	22.9	6.32	247.5	6
0	**1**	**Site 1 - 2**	20	10	22.9	6.32	245.6	6
0	**1**	**Site 1 - 3**	20	10	22.9	6.32	250	6
24	**1**	**Site 1 - 1**	1094	538	25.9	7.16	237.2	11
24	**1**	**Site 1 - 2**	1320	662	25.9	7.54	235.7	17
24	**1**	**Site 1 - 3**	1260	631	25.4	7.55	239.8	13
48	**1**	**Site 1 - 1**	1297	654	25.6	7.35	226.7	11
48	**1**	**Site 1 - 2**	1369	694	25.5	7.6	225.4	8
48	**1**	**Site 1 - 3**	1347	669	25.6	7.66	229.9	11
72	**1**	**Site 1 - 1**	1505	769	24.2	7.32	216.3	17
72	**1**	**Site 1 - 2**	1484	738	23.8	7.67	215.1	16
72	**1**	**Site 1 - 3**	1395	697	24	7.69	210.4	15
96	**1**	**Site 1 - 1**	1491	762	25.9	7.37	206.4	17
96	**1**	**Site 1 - 2**	1520	761	25.5	7.64	204.9	22
96	**1**	**Site 1 - 3**	1456	729	25.4	7.89	200	20
120	**1**	**Site 1 - 1**	1632	818	28.7	7.39	196.2	18
120	**1**	**Site 1 - 2**	1584	789	28.3	7.81	194.8	29
120	**1**	**Site 1 - 3**	1485	742	28.4	7.87	189.6	26
Δ		**Site 1 - 1**	**1612**	**808**	**5.8**	**1.07**	**-51.3**	**12**
Δ		**Site 1 - 2**	**1564**	**779**	**5.4**	**1.49**	**-50.8**	**23**
Δ		**Site 1 - 3**	**1465**	**732**	**5.5**	**1.55**	**-60.4**	**20**

Supplementary Data 2 Location 1 Weathering Analysis Data

Time (hrs)	Sample Location	Sample	EC (µS/cm)	TDS (ppm)	Temp (C)	pH	Full Container Weight	Alkalinity (ppm)
0	**2**	**Site 2 - 1**	20	10	22.9	6.32	244.1	6
0	**2**	**Site 2 -2**	20	10	22.9	6.32	244.4	6
0	**2**	**Site 2 - 3**	20	10	22.9	6.32	264.4	6
24	**2**	**Site 2 - 1**	1645	820	26	7.59	234.3	14
24	**2**	**Site 2 -2**	1248	625	25.8	7.86	234.5	10
24	**2**	**Site 2 - 3**	1422	709	25.7	7.81	235.9	11
48	**2**	**Site 2 - 1**	1781	891	25.4	7.62	224.2	15
48	**2**	**Site 2 -2**	1336	667	25.5	7.71	224	13
48	**2**	**Site 2 - 3**	1547	778	25.5	7.67	225.8	16
72	**2**	**Site 2 - 1**	1859	931	23.9	7.68	214.1	14
72	**2**	**Site 2 -2**	1450	720	23.9	7.81	213.9	18
72	**2**	**Site 2 - 3**	1621	831	24	7.69	215.6	17
96	**2**	**Site 2 - 1**	1936	967	25.6	7.66	203.9	19
96	**2**	**Site 2 -2**	1460	728	25.6	7.79	203.8	19
96	**2**	**Site 2 - 3**	1720	868	25.6	7.67	205.4	18
120	**2**	**Site 2 - 1**	1904	993	28.5	7.83	193.6	24
120	**2**	**Site 2 -2**	1505	747	28.4	7.93	193.3	25
120	**2**	**Site 2 - 3**	1798	906	28.5	7.82	195.4	26
Δ		**Site 2 - 1**	**1884**	**983**	**5.6**	**1.51**	**-50.5**	**18**
Δ		**Site 2 -2**	**1485**	**737**	**5.5**	**1.61**	**-51.1**	**19**
Δ		**Site 2 - 3**	**1778**	**896**	**5.6**	**1.5**	**-69**	**20**

Supplementary Data 3 Location 2 Weathering Analysis Data

Time (hrs)	Sample Location	Sample	EC (µS/cm)	TDS (ppm)	Temp (C)	pH	Full Container Weight	Alkalinity (ppm)
0	**3**	**Site 3 - 1**	20	10	22.9	6.32	244	6
0	**3**	**Site 3 - 2**	20	10	22.9	6.32	243.9	6
0	**3**	**Site 3 - 3**	20	10	22.9	6.32	246.5	6
24	**3**	**Site 3 - 1**	606	302	25.7	8.25	234.1	9
24	**3**	**Site 3 - 2**	954	483	25.7	8.38	233.8	14
24	**3**	**Site 3 - 3**	1191	599	25.8	8.04	236.3	20
48	**3**	**Site 3 - 1**	748	372	25.6	8.06	224	22
48	**3**	**Site 3 - 2**	1070	534	25.5	8	223.8	9
48	**3**	**Site 3 - 3**	1129	660	25.6	7.95	226.3	21
72	**3**	**Site 3 - 1**	846	413	24.2	8	213.9	20
72	**3**	**Site 3 - 2**	1129	564	24.1	7.95	213.6	21
72	**3**	**Site 3 - 3**	1374	686	24.1	7.89	216.3	24
96	**3**	**Site 3 - 1**	891	441	25.6	8.04	203.9	32
96	**3**	**Site 3 - 2**	840	417	25.6	8.05	203.6	29
96	**3**	**Site 3 - 3**	1372	689	25.4	7.97	206.1	29
120	**3**	**Site 3 - 1**	927	460	28.5	8.06	193.7	36
120	**3**	**Site 3 - 2**	1171	586	28.6	8.02	193.6	35
120	**3**	**Site 3 - 3**	1438	722	28.4	7.98	195.9	35
Δ		**Site 3 - 1**	**907**	**450**	**5.6**	**1.74**	**-50.3**	**30**
Δ		**Site 3 - 2**	**1151**	**576**	**5.7**	**1.7**	**-50.3**	**29**
Δ		**Site 3 - 3**	**1418**	**712**	**5.5**	**1.66**	**-50.6**	**29**

Supplementary Data 4 Location 3 Weathering Analysis Data

Time (hrs)	Sample Location	Sample	EC (µS/cm)	TDS (ppm)	Temp (C)	pH	Full Container Weight	Alkalinity (ppm)
0	**C**	**Control 1**	20	10	22.9	6.32	207.2	6
0	**C**	**Control 2**	20	10	22.9	6.32	207.7	6
0	**C**	**Control 3**	20	10	22.9	6.32	207.2	6
24	**C**	**Control 1**	20	11	26.9	6.67	196.7	5
24	**C**	**Control 2**	17	9	26.2	6.72	197.2	3
24	**C**	**Control 3**	20	10	26	6.65	197.2	5
48	**C**	**Control 1**	29	15	25.9	8.56	185	3
48	**C**	**Control 2**	25	12	25.9	8.22	187.1	4
48	**C**	**Control 3**	30	14	25,8	7.59	187	6
72	**C**	**Control 1**	38	19	24.5	8.28	164.7	0
72	**C**	**Control 2**	20	10	24.3	8.04	167.1	5
72	**C**	**Control 3**	22	11	24	7.9	176.3	12
96	**C**	**Control 1**	36	18	25.8	8.28	154.1	5
96	**C**	**Control 2**	23	11	25.8	7.93	157	7
96	**C**	**Control 3**	24	12	25.7	7.73	165.9	7
120	**C**	**Control 1**	43	22	28.8	7.66	143.3	4
120	**C**	**Control 2**	24	12	28.8	7.64	146.4	3
120	**C**	**Control 3**	23	12	28.8	7.54	155.9	9
Δ		**Control 1**	**23**	**12**	**5.9**	**1.34**	**-63.9**	**-2**
Δ		**Control 2**	**4**	**2**	**5.9**	**1.32**	**-61.3**	**-3**
Δ		**Control 3**	**3**	**2**	**5.9**	**1.22**	**-51.3**	**3**

Supplementary Data 5 Control Weathering Analysis Data

Sample	Site 1 - 1	Site 1 - 2	Site 1 - 3	Site 2 - 1	Site 2 -2	Site 2 - 3	Site 3 - 1	Site 3 - 2	Site 3 - 3
Material Weight (kg)	0.0547	0.0540	0.5860	0.5140	0.0528	0.0558	0.0514	0.0516	0.0540
Material Volume (m3)	3.04E-08	3.00E-08	3.26E-07	2.86E-07	2.93E-08	3.10E-08	2.86E-08	2.87E-08	3.00E-08
>6.7mm	0.242	0.242	0.242	0.375	0.375	0.375	0.341	0.341	0.341
4.0mm - 6.7mm	0.158	0.158	0.158	0.168	0.168	0.168	0.129	0.129	0.129
2.00mm - 4.00mm	0.179	0.179	0.179	0.154	0.154	0.154	0.114	0.114	0.114
0.42mm - 2.00mm	0.342	0.342	0.342	0.225	0.225	0.225	0.269	0.269	0.269
0.0075mm - 0.42mm	0.080	0.080	0.080	0.077	0.077	0.077	0.147	0.147	0.147
Particle Volume >6.7mm (m3)	*3.35E-08*	*3.35E-08*	*3.35E-08*	*3.35E-08*	*3.35E-08*	*3.35E-08*	*3.35E-08*	*3.35E-08*	*3.35E-08*
Particle Volume 4.0mm (m3)	*4.19E-09*	*4.19E-09*	*4.19E-09*	*4.19E-09*	*4.19E-09*	*4.19E-09*	*4.19E-09*	*4.19E-09*	*4.19E-09*
Particle Volume 2.00mm (m3)	*3.88E-11*	*3.88E-11*	*3.88E-11*	*3.88E-11*	*3.88E-11*	*3.88E-11*	*3.88E-11*	*3.88E-11*	*3.88E-11*
Particle Volume 0.42mm (m3)	*2.21E-13*	*2.21E-13*	*2.21E-13*	*2.21E-13*	*2.21E-13*	*2.21E-13*	*2.21E-13*	*2.21E-13*	*2.21E-13*
Particle Volume 0.075mm (m3)	*2.21E-13*	*2.21E-13*	*2.21E-13*	*2.21E-13*	*2.21E-13*	*2.21E-13*	*2.21E-13*	*2.21E-13*	*2.21E-13*
Roadway Volume >6.7mm (m3)	7.35E-09	7.26E-09	7.88E-08	1.07E-07	1.10E-08	1.16E-08	9.74E-09	9.78E-09	1.02E-08
Roadway Volume 4.0mm -	4.80E-09	4.74E-09	5.14E-08	4.80E-08	4.93E-09	5.21E-09	3.68E-09	3.70E-09	3.87E-09
Roadway Volume 2.00mm -	5.44E-09	5.37E-09	5.83E-08	4.40E-08	4.52E-09	4.77E-09	3.26E-09	3.27E-09	3.42E-09
Roadway Volume 0.42mm -	1.04E-08	1.03E-08	1.11E-07	6.43E-08	6.60E-09	6.98E-09	7.68E-09	7.71E-09	8.07E-09
Roadway Volume 0.0075mm -	2.43E-09	2.40E-09	2.60E-08	2.20E-08	2.26E-09	2.39E-09	4.20E-09	4.21E-09	4.41E-09
Particle Count >6.7mm	2.19E-01	2.17E-01	2.35E+00	3.20E+00	3.28E-01	3.47E-01	2.91E-01	2.92E-01	3.05E-01
Particle Count 4.0mm - 6.7mm	1.15E+00	1.13E+00	1.23E+01	1.15E+01	1.18E+00	1.24E+00	8.79E-01	8.83E-01	9.24E-01
Particle Count 2.00mm -	1.40E+02	1.38E+02	1.50E+03	1.13E+03	1.16E+02	1.23E+02	8.39E+01	8.42E+01	8.82E+01
Particle Count 0.42mm -	4.70E+04	4.64E+04	5.04E+05	2.91E+05	2.99E+04	3.16E+04	3.48E+04	3.49E+04	3.65E+04
Particle Count 0.0075mm -	1.10E+04	1.09E+04	1.18E+05	9.95E+04	1.02E+04	1.08E+04	1.90E+04	1.91E+04	2.00E+04
Particle Area >6.7mm (m2)	*1.41E-04*	*1.41E-04*	*1.41E-04*	*1.41E-04*	*1.41E-04*	*1.41E-04*	*1.41E-04*	*1.41E-04*	*1.41E-04*
Particle Area 4mm (m2)	*5.03E-05*	*5.03E-05*	*5.03E-05*	*5.03E-05*	*5.03E-05*	*5.03E-05*	*5.03E-05*	*5.03E-05*	*5.03E-05*
Particle Area 2mm (m2)	*1.26E-05*	*1.26E-05*	*1.26E-05*	*1.26E-05*	*1.26E-05*	*1.26E-05*	*1.26E-05*	*1.26E-05*	*1.26E-05*
Particle Area 0.42mm (m2)	*5.54E-07*	*5.54E-07*	*5.54E-07*	*5.54E-07*	*5.54E-07*	*5.54E-07*	*5.54E-07*	*5.54E-07*	*5.54E-07*
Particle Area 0.0.075mm (m2)	*1.77E-08*	*1.77E-08*	*1.77E-08*	*1.77E-08*	*1.77E-08*	*1.77E-08*	*1.77E-08*	*1.77E-08*	*1.77E-08*
Surface Area >6.7mm (m2)	3.09E-05	3.06E-05	3.32E-04	4.51E-04	4.63E-05	4.89E-05	4.10E-05	4.11E-05	4.31E-05
Surface Area 4.0mm - 6.7mm	5.76E-05	5.69E-05	6.17E-04	5.76E-04	5.91E-05	6.25E-05	4.42E-05	4.44E-05	4.64E-05
Surface Area 2.00mm - 4.00mm	1.76E-03	1.74E-03	1.89E-02	1.42E-02	1.46E-03	1.55E-03	1.05E-03	1.06E-03	1.11E-03
Surface Area 0.42mm - 2.00mm	2.61E-02	2.57E-02	2.79E-01	1.61E-01	1.66E-02	1.75E-02	1.93E-02	1.93E-02	2.02E-02
Surface Area0.0075mm -	1.94E-04	1.92E-04	2.08E-03	1.76E-03	1.81E-04	1.91E-04	3.36E-04	3.37E-04	3.53E-04
Total Surface Area available	**0.0281**	**0.0278**	**0.3012**	**0.1782**	**0.0183**	**0.0193**	**0.0207**	**0.0208**	**0.0218**

Supplementary Data 6 Available Weathering Surface Area Calculation Table